Nitrone-Trolox conjugate as an inhibitor of lipid oxidation: Towards synergistic antioxidant effects

Larissa Socrier, Marie Rosselin, Ana Milena Gomez Giraldo, Benjamin Chantemargue, Florent Di Meo, Patrick Trouillas, Grégory Durand, Sandrine Morandat

Nitrone-Trolox conjugate as an inhibitor of lipid oxidation: Towards synergistic antioxidant effects

Larissa Socrier[a,*], Marie Rosselin[b], Ana Milena Gomez Giraldo[a], Benjamin Chantemargue[c, d], Florent Di Meo[c], Patrick Trouillas[c, d], Grégory Durand[b] and Sandrine Morandat[a]

[a]Sorbonne Universités, Université de technologie de Compiègne. CNRS, Génie Enzymatique et Cellulaire, FRE 3580. Centre de recherches Royallieu, CS 60319 − 60203 Compiègne cedex, France;

[b]Institut des Biomolécules Max Mousseron (UMR 5247 CNRS-Université Montpellier-ENSCM) & Avignon University, Equipe Chimie Bioorganique et Systèmes Amphiphiles, 301 rue Baruch de Spinoza, F-84916 Avignon Cedex 9, France ;

[c]INSERM, Univ. Limoges, IPPRITT, U1248, Faculty of Pharmacy, 2 rue du Dr Marcland, 87025 Limoges, France;

[d]RCPTM, Palacký University, Faculty of Sciences, Šlechtitelů 27, 78371, Olomouc, Czech Republic

*Corresponding author: las218@lehigh.edu, Tel: +1 (610) 758 5328

Present address: Lehigh University, Department of Physics. 416 Lewis Laboratory, 16 Memorial Drive East. Bethlehem, Pennsylvania, 18 015. USA.

Abstract

Free radical scavengers like α-phenyl-*N*-*tert*-butylnitrone (PBN) and 6-hydroxy-2,5,7,8-tetramethylchroman-2-carboxylic acid (Trolox) have been widely used as protective agents in various biomimetic and biological models. A series of three amphiphilic Trolox and PBN derivatives have been designed by adding to those molecules a perfluorinated chain as well as a sugar group in order to render them amphiphilic. In this work, we have studied the interactions between these derivatives and lipid membranes to understand how they influence their ability to prevent membrane lipid oxidation. We showed the derivatives better inhibited the AAPH-induced oxidation of 1,2-dilinoleoyl-sn-glycero-3-phosphocholine (DLiPC) small unilamellar vesicles (SUVs) than the parent compounds. One of the derivatives, bearing both PBN and Trolox moieties on the same fluorinated carrier, exhibited a synergistic antioxidant effect by delaying the oxidation process. We next investigated the ability of the derivatives to interact with DLiPC membranes in order to better understand the differences observed regarding the antioxidant properties. Surface tension and fluorescence spectroscopy experiments revealed the derivatives exhibited the ability to form monolayers at the air/water interface and spontaneously penetrated lipid membranes, underlying pronounced hydrophobic properties in comparison to the parent compounds. We observed a correlation between the hydrophobic properties, the depth of penetration and the antioxidant properties and showed that the location of these derivatives in the membrane is a key parameter to rationalize their antioxidant efficiency. Molecular dynamics (MD) simulations supported the understanding of the mechanism of action, highlighting various key physical-chemical descriptors.

Key words: model membranes; lipid oxidation; amphiphilic nitrone; Trolox; antioxidant; synergism

1. Introduction

Reactive oxygen species (ROS) are produced in living organisms and are involved in several important biological processes such as signaling pathways [1], antimicrobial defense [2] or cell adhesion [3]. However, the deregulation of physiological processes as well as the exposure to environmental factors like pollution, radiations or tobacco smoke may favor an overproduction of ROS [4], which unbalance the redox status of cells and lead to oxidative stress. Because of their ability to damage biomolecules, in particular membrane polyunsaturated lipids which are degraded through a reaction named lipid peroxidation [5]; ROS are involved in the early stages of various diseases [6–8] as well as the deterioration of cosmetic [9], food [10,11] and pharmaceutical supplies [12].

In order to limit the deleterious effects of ROS, living organisms use several antioxidant defense systems that are either endogenous − mainly enzymes but also small molecules such as glutathione − or exogenous [13]. Exogenous antioxidants, essentially polyphenols and vitamins, come from food. To improve their properties, bioinspired molecules have been developed based on these natural compounds. In this regard, Trolox (6-hydroxy-2,5,7,8-tetramethylchroman-2-carboxylic acid), a water soluble analog of α-tocopherol, has been used to prevent apoptosis [14], *in vitro* or *ex vivo* ischemia [15] and membrane lipid oxidation [16]. Trolox is also used as a reference in the evaluation of antioxidant activities. Namely, the Trolox equivalent antioxidant capacity (TEAC) parameter measures the potency of a given antioxidant. TEAC also allows the comparison of antioxidant efficiency of food matrices and beverages, for which isolation of molecules can rarely been achieved [17,18]. Also, because of their enhanced reactivity against free radicals, spin trapping agents can be used as free radical scavengers [19]. Among them, α-phenyl-*N*-*tert*-butylnitrone (PBN) is one of the most popular. PBN was initially used in electron spin resonance (ESR) experiments for the detection of free radicals under chemical and biological environments, however, it has later been used in biological models as an antioxidant [20,21]. Although PBN has the advantage of being a non-toxic chemically stable antioxidant with a half-life of six hours in animals [22], it presents like Trolox a poor ability to remain inside

membranes. To create antioxidants with a greater hydrophobicity and therefore a better affinity for membranes, several molecules deriving from PBN and Trolox have been designed. For instance, Ayuso *et al.* [23], as well as Choteau *et al.* [24], reported the synthesis of PBN derivatives bearing a cholesterol moiety. In both cases, these authors demonstrated that compared to PBN, the derivatives presented an enhanced protective activity against stroke and retina light-induced damages, respectively. Besides the need of increasing the affinity for the membrane, a strategy that has gained attention is to combine two (or more) antioxidant moieties in a single molecule [25]. In this regard, Trolox was combined to lipoic acid [26], silybin [27] as well as a nitric oxide synthase inhibitor [28]. Along the same line, Trolox and PBN amphiphilic derivatives [29,30] have recently been synthesized. They bear, on one hand, a perfluorinated chain to increase hydrophobicity without inducing a cytolytic effect [31] and on the other hand, a sugar group to maintain water solubility (Fig. 1).

In the present work, we have studied the antioxidant properties of these derivatives related to their capacity to interact with lipid membranes, which in turn has allowed unraveling their antioxidant properties by using biomimetic systems. The antioxidant action at the membrane was evaluated by performing Langmuir monolayers and lipid peroxidation inhibition assays. Surface tension and fluorescence spectroscopy experiments showed the capacity of these derivatives to interact with membrane lipids, with respect to the parent compounds (Trolox and PBN). The nature of the free-radical scavenger moieties and their location in the membranes were analyzed as key parameters to rationalize the antioxidant activity of these derivatives, which was supported by molecular dynamics (MD) simulations.

2. Materials and methods

2.1. Chemicals

Vials of 1,2-dilinoleoyl-*sn*-glycero-3-phosphocholine (DLiPC) powder were purchased from Avanti Polar Lipids (Alabaster, AL, USA). 2,2'-azo-bis(2-amidinopropane)dihydrochloride (AAPH), 4-(2-hydroxyethyl)piperazine-1-ethanesulfonic acid (Hepes), (±)-6-hydroxy-2,5,7,8-tetramethylchromane-2-carboxylic acid (Trolox) and α-phenyl-*N*-*tert*-butylnitrone (PBN) were purchased from Sigma (St. Louis, MO, USA). FAPBN [29], FATx [29] and FATxPBN [30] were synthesized according to the procedure previously published.

The water used in all assays was purified using a Millipore filtering system (Bedford, MA, USA), yielding ultrapure water (18.2 MΩ×cm). Stock solutions of DLiPC were prepared by dissolving the DLiPC powder contained in the vials in chloroform or hexane/ethanol 9:1 (v/v) for the preparation of vesicles and monolayers, respectively. The antioxidants were dissolved in chloroform and ethanol for the experiments involving vesicles and monolayers, respectively. log*P* values were calculated with the software ChemSketch version 14.01, Advanced Chemistry Development, Inc. (Toronto, ON, Canada).

2.2. Preparation of DLiPC vesicles

DLiPC alone (control assay) and DLiPC/antioxidant mixtures dissolved in chloroform were dried under a stream of nitrogen and then kept under high vacuum for 2 hours to obtain a solvent-free film. The dried film was then dispersed in Hepes buffer to obtain a solution of DLiPC multilamellar vesicles (MLVs) at a concentration of 0.5 mg/mL. Small unilamellar vesicles (SUVs) were obtained by sonicating MLVs to clarity (3 cycles of 2 min 30 s) with a 500 W titanium probe sonicator at 33 % of the maximal power from Fisher Bioblock Scientific (Illkirch-Graffenstaden, Grand-Est, France). To limit oxidation due to heat and light, sonication was performed in the dark and samples were kept in an ice bath. Then, the SUVs solution was filtered on 0.2 µm Acrodisc® from Pall Life Sciences (Port Washington, NY, USA) to remove titanium particles. To prepare large unilamellar vesicles (LUVs), the MLVs suspension was

extruded 19 times at room temperature through a 200 nm nuclepore polycarbonate membrane filter from Avestin Inc. (Ottawa, Ontario, Canada) with a syringe-type extruder from Avanti Polar lipids Inc. (Alabaster, AL, USA). SUVs and LUVs size distribution were determined by dynamic light scattering with a Zetasizer Nano-S from Malvern Instruments (Malvern, Worcestershire, UK). The sizes were on average 60 nm after sonication and 190 nm after extrusion. The distributions were unimodal.

2.3. Evaluation of the antioxidant efficiency of the fluorinated derivatives

The antioxidant efficiency of the non-modified compounds as well as the derivatives was assessed by evaluating their ability to protect lipid vesicles from oxidation. Because they are frequently used to evaluate the antioxidant properties of various molecules [32,33], SUVs were chosen to perform these experiments. DLiPC SUVs (control assay) and DLiPC SUVs containing fluorinated derivatives, Trolox or PBN at different concentrations were prepared in Hepes buffer as described in section 2.2. The vesicles were diluted to a final DLiPC concentration of 0.1 mg/mL AAPH, an azo compound widely used in biochemical reactions to study lipid oxidation [34], was added at a final concentration of 2 mM and the samples were immediately incubated at 37°C. The heat triggered the degradation of AAPH into peroxyl radicals that initiated the oxidation of the vesicles [35]. As they absorb ultraviolet light between 230 and 235 nm [36] and since they constitute the primary oxidation products of polyunsaturated lipids [5,37], conjugated dienes were used as an indicator of lipid oxidation. Their appearance was followed by measuring the absorbance at 234 nm with a Specord S300 UV–VIS spectrophotometer (Jena, Thuringia, Germany). The values were normalized to zero by subtracting the initial absorbance (0.8 ± 0.2). The results are expressed as percentages of peroxidation, calculated as follows:

$$Lipid\ oxidation\ (\%) = \frac{Absorbance_{sample}}{Absorbance\ max_{Control}} * 100\ (eq.3)$$

The curves were fitted by applying a dose-response model with variable slope with the software GraphPadPrism version 6.00 for Windows (La Jolla, CA, USA).

To further characterize the differences in the antioxidant efficiency of the derivatives, we calculated the lag time of oxidation as follows:

$$lag\ time = time_{10/20\%}^{sample} - time_{10/20\%}^{control}\ (eq.4)$$

where $time_{10/20\%}$ corresponds to the time required to reach 10 or 20 % of oxidation for the DLiPC SUVs containing 6,4 µM of antioxidant (5 %, mol/mol compared to DLiPC) and for the pure DLiPC vesicles (control assay).

2.4. Surface pressure experiments

All the experiments were performed at constant temperature (21.0 ± 0.1°C). The film balance was built by Nima (Coventry, West Midlands, England) for adsorption experiments on a small Teflon dish. The dish (surface=19.6 cm²) was equipped with a Wilhelmy-type pressure measuring system. In these experiments, we used a subphase buffer of 62 mL continuously stirred with a magnetic stirrer spinning at a rate of 100 rpm. The buffer contained 10 mM of Hepes, 150 mM of NaCl and was adjusted at a pH of 7.4. To prepare Gibbs monolayers, the compounds – dissolved in ethanol – were injected in the subphase at two ranges of concentrations: from 1 to 40 µM for PBN and Trolox, from 0.0625 to 10 µM for the fluorinated derivatives. Surface tension was recorded during 5 min after the injection.

In order to study the adsorption of the compounds to DLiPC monolayers, DLiPC was dissolved in hexane/ethanol 9:1 (v/v) and spread at the air-water interface to reach the desired surface pressure. As soon as the initial surface pressure was stabilized (~ 15 min), the compounds were injected into the subphase at a final concentration of 50 nM. Their adsorption at the air-lipid buffer interface was then followed by measuring the variation of surface pressure during 15 minutes. As monolayers of unsaturated lipids tend to oxidize in contact with air [38,39], we made sure the experiments lasted less than 40 minutes to avoid a loss of stability due to lipid oxidation. A control experiment was also performed by injecting ethanol in the subphase, which produced no significant perturbation of the surface pressure. The binding parameters [40,41] were determined with the calculator available on the

following webpage: http://www.crchudequebec.ulaval.ca/BindingParametersCalculator/. The kinetics of adsorption of the antioxidants in DLiPC monolayers was studied by fitting the data to the following equation [42,43]:

$$ln[(\Pi_\infty - \Pi_t)/(\Pi_\infty - \Pi_i)] = kt \ (eq. 5)$$

where Π_∞ designates the equilibrium surface pressure after the injection of the antioxidants in the subphase of the monolayer, Π_i the initial surface pressure of the monolayer, Π_t the surface pressure at a time t and k the rate coefficient. Π_∞-Π_i can also be defined as $\Delta\Pi$, which designates the maximum increase of surface pressure induced by the penetration of the antioxidants in DLiPC monolayers.

2.5. Effect of the antioxidants on the permeability of the membrane

The ability of the fluorinated antioxidants to permeabilize DLiPC vesicles was measured with the calcein release assay. LUVs were chosen instead of SUVs in order to encapsulate larger amounts of calcein and because the extrusion process allows the elimination of the concentric layers of MLVs without releasing the encapsulated calcein. DLiPC LUVs were prepared as described in section 2.2 with Hepes buffer containing 35 mM calcein. Free calcein was separated from encapsulated calcein by gel filtration on a sepharose 4B column equilibrated with Hepes buffer. Lipids were quantified with the method developed by Stewart [44]. The solution containing calcein loaded LUVs was diluted to a final concentration of 10 µM lipids in Hepes buffer. Fluorinated antioxidants dissolved in ethanol were added after 5 min at a ratio of 5 % (mol/mol) compared to DLiPC. Fluorescence measurements were performed at 21 °C as soon as the LUVs were prepared, immediately after the addition of fluorinated derivatives and after 30, 60 min and 120 min of incubation with a Varian Cary Eclipse fluorescence spectrophotometer (Santa Clara, CA, USA). We used excitation and emission wavelengths of 490 and 520 nm respectively. Triton X-100 was added after two hours in order to release the total amount of encapsulated calcein. The intrinsic fluorescence of fluorinated antioxidants at 520 nm was verified and

the values we found were not significant. Release percentages were calculated with the following equation:

$$Calcein\ release\ (\%) = \frac{(F_{1-}F_0)}{(F_{Tot} - F_0)} * 100\ (eq.2)$$

where F_0 designates the fluorescence of the LUVs measured in absence of fluorinated derivatives, F_1 the fluorescence of the LUVs measured after addition of fluorinated derivatives and F_{Tot} the fluorescence measured after addition of Triton X100 that triggers the release of the encapsulated calcein.

2.6. Theoretical methodology

Two DLiPC membranes made of 128 and 72 lipids each, were created using the membrane bilayer builder from the CHARMM-GUI server [45]. The membranes were solvated with a hydration number of 35 water molecules per lipid. Na^+ and Cl^- ions were added at a 0.154 M concentration, ensuring the neutrality of the system. The DLiPC lipids were described using the lipid 11 force field [46]. The force field parameters for the different compounds (Trolox, anionic Trolox, PBN, FATx, FAPBN, FATxPBN) were derived from the Generalized Amber Force Field version 2 (GAFF2) [47–49] for all moieties but the sugars, which were described by the GLYCAM force field [50], using the antechamber package [51]. FATx, FAPBN and FATxPBN were built using a building block approach (*i.e.*, considering the β-D-galactopyranosyl, 2,6-diaminohexanoyl, 1-amino-dodecafluorooctanyl, Trolox and PBN residues). Atomic charges were derived from RESP (Restrained fit of Electro Static Potential) based on the calculations achieved within the Density Functional Theory (DFT) formalism with the IEFPCM-B3LYP/cc-pVDZ method in diethylether [52], accounting for the chemical environment in the building block approach. The DFT calculations and the atomic charge fitting were performed with the Gaussian 09, RevA [53] and R.E.D. III [54] softwares, respectively. The three-point TIP3P water model [55] was used to describe water molecules. The anionic Trolox was used because, regarding the low pKa of the carboxylic moiety, Trolox exists in its deprotonated form in the bulk water, and both (neutral and

anionic) forms may co-exist in the bilayer. However, regarding insertion in membrane, no significant differences were observed between the two forms, therefore the results have not been detailed.

MD simulations were carried out using CPU-Particle-Mesh Ewald (PME) [56] MD codes available in Amber16 [57,58], and according to the following procedure: minimization of water molecules prior to minimization of the entire system to prevent from steric clash; slow thermalization of the water molecules up to 100 K in the (N,V,T) ensemble for 200 ps; thermalization of the whole system to the final temperature (310 K) for 500 ps in the (N,P,T) ensemble; equilibration of the system for 5 ns (N,P,T) MD simulations. Productions of 600 ns (N,P,T) MD simulations were then achieved. PME MD simulations were carried out using the SHAKE algorithm [59] on H-bonds and a 10 Å non covalent interaction cut-off for both Coulomb and van der Waals interactions. The temperature was maintained using the Langevin dynamics [60] with a collision frequency of 1 ps^{-1}. Semi-isotropic pressure scaling with constant surface tension in the xy-plane perpendicular to the membrane normal (z-axis) was used with Berendsen barostat [61], in which the pressure relaxation time was set to 1 ps.

The compounds were inserted in the bulk water of the equilibrated membrane systems, preventing from steric clash with water molecules. MD simulations of 600 ns were then carried out with all the compounds; the total MD simulation time for the six derivatives was 3.6 µs. The analyses were performed along the last 300 ns, which allowed a robust sampling of structural properties, *i.e*., after the equilibrium was reached. They were carried out using the cpptraj software [62]. The positions of the center of mass (COM) or key moieties of the different compounds in membranes are given with respect to the middle of the bilayer (*i.e.,* z-component of the vector originated at the COM of the lipid bilayer and pointing towards the COM of the compound). The orientation of the compounds in the lipid bilayer was assessed by the α-angle between the z-axis and the normal vector(s) defined for each compound (see supplemental data).

233 2.7. Statistical analysis

234 Statistical analysis was performed with the software GraphPadPrism version 6.0 for Windows (La
235 Jolla, CA, USA). Since our samples are small (N<30) and because the values do not follow a normal
236 distribution, the Mann-Whitney/Wilcoxon test was carried out to compare the combination indexes of
237 the compounds at low (*i.e.* less than 1 µM) and high (*i.e.* more than 1 µM) concentrations. *p* values <
238 0.05 were considered as statistically significant.

239

3. Results

3.1. Fluorinated derivatives are efficient to limit lipid peroxidation

In order to evaluate the antioxidant efficiency of the compounds, DLiPC SUVs containing the parent compounds or the fluorinated derivatives were prepared and incubated with AAPH. Oxidation percentages were calculated with eq.3 as described in section 2.3 and reported over time. In absence of antioxidant we observed an immediate increase of the percentages of oxidation. The exponential phase was reached after 10 min and the percentages of oxidation kept increasing until reaching a plateau at 60 min (Fig. 2A). This increase is due to the formation of conjugated dienes which are the primary products of lipid oxidation [5,37], and which in turn drive the beginning of the kinetics. Consequently, after 80 min, the percentages of lipid oxidation in absence of antioxidants decreased, as the oxidation process continued beyond the conjugated dienes stage. Namely, conjugated dienes were progressively replaced by secondary peroxidation products that are not detected at 234 nm. With increasing concentrations of FATxPBN, oxidation percentages firstly increased slower than the control, which suggests an ability of FATxPBN to slow down the oxidation process. The exponential phase started after 60 min, at a higher level of oxidation than the control, causing the oxidation percentages to go over 100 % after 100 min. Also, we noticed a gradual decrease of oxidation percentages, showing a dose-dependent antioxidant efficiency of FATxPBN (Fig. 2A). Similar tendencies, although they were less pronounced, were observed with Trolox, FATx and FAPBN (Fig. S1).

To better compare the antioxidant efficiencies, we reported the percentages of oxidation at 80 min (*i.e.,* the time required to reach the plateau in the absence of antioxidant) versus the antioxidant concentration (Fig. 2B-F). For FATxPBN and FATx, concentrations ranging from 1.6 to 6.4 µM appeared sufficient to reach the maximal antioxidant efficiency. FAPBN was significantly less efficient as saturation was reached with a concentration of 38.4 µM. No significant antioxidant efficiency was observed for PBN, even at high concentrations (*i.e.* 25.6-38.4 µM). Trolox, FATxPBN, FATx and FAPBN presented IC_{50} (concentration required to half-reduce the oxidation in absence of antioxidant) values of

4.0, 0.6, 0.9, and 29.5 µM, respectively, whereas no IC_{50} could be determined for PBN. The better capacity of Trolox to inhibit lipid oxidation in comparison to PBN agrees with previous work [30], where we showed that Trolox was more efficient than PBN to scavenge $ABTS^{+\bullet}$ radicals. In the present work, all three fluorinated derivatives exhibited lower IC_{50} than their parent compounds. Indeed, FATxPBN and FATx exhibited IC_{50} values ~ 5 times lower than Trolox (0.6 and 0.9 µM versus 4.0 µM). FAPBN displayed an IC_{50} of 29.5 µM while PBN presented no IC_{50}.

To better compare the most efficient derivatives (*i.e.* FATxPBN and FATx), we determined the lag times (Fig. 3), which represent the time required to reach either 10 or 20 % lipid peroxidation for DLiPC SUVs containing 5 % (mol/mol, concentration at which the antioxidant efficiency was optimal) of antioxidant. Except for PBN and FAPBN at 20% oxidation (1.5 ± 2.0 and 6.0 ± 1.0 min, respectively), the lag times of the fluorinated antioxidants did not significantly differ compared to that of the parent compounds. In the case of FATxPBN, the lag time to reach 10 and 20 % of oxidation was significantly higher than the two other derivatives, suggesting that this molecule has a different kinetic inhibition process which efficiently delayed the oxidation process. These data confirmed a significantly improved antioxidant efficiency of the fluorinated antioxidants with respect to the parent compounds.

3.2. Interactions of the antioxidants with DLiPC membranes

3.2.1. Interfacial behavior of the antioxidants

To characterize the amphiphilicity of the compounds and gain information on their hydrophobic properties, we measured their ability to adsorb at the air-buffer interface. Increasing concentrations were injected in the subphase and the surface tension was recorded continuously to assess the formation of a Gibbs monolayer at the interface. The injection of 1, 5, 10, 20 and 30 µM of Trolox and PBN exhibited only a poor effect on the surface pressure as the variations of surface pressure ($\Delta\Pi$) recorded were ranging between 0 and 3 mN/m (Fig. S2). Conversely, the fluorinated antioxidants presented a high surface activity since the injection of 0.1 µM was sufficient to observe a significant

surface activity (Fig. 4). A maximal surface activity of ~ 40 mN/m was reached at only 1 µM for FATxPBN and FATx and at 3 µM for FAPBN, indicating that both FATxPBN and FATx are more hydrophobic than FAPBN. Higher concentrations (*i.e.* 5 and 10 µM) were also tested and the $\Delta\Pi$ values remained close to 40 mN/m, reflecting the formation of stable monolayers at the air-water interface.

The micellization was previously studied and results showed that while the parent compounds exhibit no critical micellar concentration (cmc); FATxPBN and FAPBN have cmc values of 10 and 51 µM, respectively [30]. In accordance with the cmc values, the three fluorinated antioxidants exhibited log*P* values significantly higher than the parent compounds (Fig. 1). The higher hydrophobicity of Trolox over PBN was clearly observed, with log*P* values of 3 and 1.3, respectively. This was also observed when comparing FATx and FAPBN that present log*P* values of 3.8 and 2, respectively. The same tendency was observed with the experimentally-determined logk'_w values previously reported [30]. FATxPBN and FATx exhibited logk'_w values ~ 5 times higher than Trolox when that of FAPBN was 3 times higher than PBN. This confirms the strong contribution of the perfluorinated chain to the overall hydrophobicity of amphiphilic molecules leading therefore to low cmc values [63]. Altogether, the higher hydrophobic character of the fluorinated antioxidants compared to the parent compounds suggest a better ability to interact with the hydrophobic core of the membrane, which may explain the more pronounced antioxidant efficiency previously observed.

3.2.2. Interactions with an unsaturated phospholipid

Oxidative stress as well as Gibbs monolayers experiments revealed significant discrepancies regarding the hydrophobic properties of fluorinated antioxidants as well as their ability to prevent membrane lipid oxidation. To evaluate their ability to interact with membranes and understand those differences of efficiency, we performed adsorption assays at lipid monolayers. DLiPC monolayers were prepared at different initial pressures and the derivatives were injected into the subphase. The variation of pressure was recorded to evaluate the ability of the derivatives to modify the surface activity of the monolayer. Due to the strong surface activity of the fluorinated antioxidants and the

formation of aggregates above the cmc, the derivatives were injected in the subphase of the monolayers at a final concentration of 0.05 µM; a concentration significantly lower than their cmc at which they all presented a negligible surface activity (see Fig. 4). The variation of pressure ($\Delta\Pi$) was reported over the initial surface pressure (Π_i) in order to determine the binding parameters of the compounds [40]. The injection of the parent compounds had little effect on the surface pressure, as $\Delta\Pi$ remains below 3 mN/m independently of the initial pressure (Fig. S3). Conversely, the injection of the fluorinated antioxidants (Fig. 5A-C) caused an immediate increase of the surface pressure and $\Delta\Pi$ decreased when the initial pressure was increased. The synergy factor was calculated by adding one to the value of the slope of the regression curve (Table 1). All the compounds presented positive synergy factors, indicating a favorable binding of the compounds to DLiPC membranes. Also, linear regression provided the maximal insertion pressure (MIP), highlighting the highest pressure at which fluorinated antioxidants can penetrate monolayers [40]. As reported in Table 1, FATxPBN, FATx and FAPBN exhibited MIPs of 52.2, 48.6 and 37.6 mN/m, respectively. Because all the MIPs are higher than the average lateral pressure in biological membranes − ~ 30mN/m [64] −, one can conclude that fluorinated antioxidants can penetrate bilayers under physiological conditions.

Since the lower MIP of FAPBN may indicate a less pronounced affinity for DLiPC monolayers [41], another parameter named $\Delta\Pi_0$ can be determined to gain information on the ability of the fluorinated antioxidants to partition into DLiPC membranes [40]. $\Delta\Pi_0$ is determined by performing an extrapolation on Fig. 5 from an initial surface pressure of 0 mN/m and corresponds to the intersection of the linear regression with the y-axis. We performed an extrapolation at the average lateral pressure of membranes − *i.e.* 30 mN/m [64] − to determine $\Delta\Pi_{30}$, which is related to the quantity of compound associated to the monolayer. As reported in Table 1, FATxPBN and FATx exhibited $\Delta\Pi_{30}$ values ~ 4 times higher than FAPBN (10.0 and 9.0 versus 2.1 mN/m), indicating that greater amounts of FATxPBN and FATx spontaneously penetrated the membrane in comparison to FAPBN.

Fitting the data recorded at 30 mN/m with eq.5 allowed us to determine the rate of penetration (k) of the fluorinated antioxidants in DLiPC monolayers at the average lateral pressure of membranes, as described in [43]. The plot yielded three linear regions (Fig. 6). The first linear region corresponds to the stabilization of the lipid monolayer in absence of antioxidant, the second one to the penetration of the antioxidants in the monolayer and the third one to the rearrangement between the lipids and the antioxidants in the monolayer [42]. The rate of penetration was determined by calculating the slope of the second linear region (Table 1). FATx and FATxPBN present k values twice as important as FAPBN, showing they penetrate the membrane faster than FAPBN. This result, in accordance with the MIP and $\Delta\Pi_{30}$ values, underlines the effect of the fluorinated chain, which has increased the affinity of the parent compounds for DLiPC.

Although our results indicate the fluorinated antioxidants interact favorably with DLiPC membranes, we are aware that hydrogenated and fluorinated lipids may not be miscible [65,66]. Nevertheless, there is a general consensus among the community that fluorinated and hydrogenated surfactants are miscible, however whether they do mix completely or only partially is still subject to debate [67]. Several reports in the literature suggests various degrees of miscibility between fluorinated and hydrogenated detergents and therefore different scenarios of mixing leading to: (i) the formation of one type of mixed micelles [68]; (ii) the demixing of the two leading to the coexistence of two types of micelles [69] or (iii) both, depending on the mixing ratio [70,71]. In our case, it is worth mentioning that FATx and FATxPBN reached their maximum antioxidant efficiency at concentrations ranging from 1.6 to 6.4 µM (*i.e*. molar ratios ranging from 1.25 to 5 % in comparison to DLiPC, Fig. 2D-E). These ratios are sufficiently low to expect only slightly perturbations of the membrane and prevent miscibility issues. Conversely, FAPBN was not efficient at low concentrations and 38.4 µM (*i.e*. 30 % molar ratio) was required to reach a significant antioxidant efficiency (Fig. 2F). The low antioxidant efficiency combined with the poor affinity for membranes as well as the possible impact of a high concentration

363 in membranes highlight the fact that FAPBN presents less interest than the two other fluorinated
364 antioxidants.

365 3.3. The fluorinated antioxidants do not modify the membrane's structure

366 We performed calcein release experiments to evaluate the impact of the fluorinated antioxidants
367 on the membrane integrity. DLiPC LUVs containing calcein were prepared and the fluorinated
368 antioxidants were added to the samples and fluorescence was measured during 2 hours to evaluate
369 the calcein leakage. The fluorinated antioxidants were introduced at a 5 % molar ratio in comparison to
370 DLiPC since at this concentration the antioxidant effect we observed was maximal in the case of
371 FATxPBN and FATx (see Fig. 2). In order to stay consistent, FAPBN was tested with the same
372 concentration although its antioxidant efficiency was limited at low concentrations. Tests of
373 permeability with higher concentrations would have not been relevant from a physiological point of
374 view since an antioxidant is supposed to be efficient at low concentrations [72]. In all cases, the
375 addition of the derivatives caused a weak leakage from the LUVs, with however a percentage of
376 leakage below 5 % during the entire experiment (Fig. S4). The addition of Triton X100 after two hours
377 caused a significant increase of the fluorescence intensity due to the release of the total amount of
378 encapsulated calcein. Because the injection of the derivatives did not significantly modify calcein
379 leakage, we concluded that their insertion has no significant effect on the structure of the membrane.

380 Regarding the interactions between fluorinated surfactants and phospholipids, it is generally
381 admitted that fluorinated surfactants do not solubilize membranes and therefore they have been
382 successfully used to solubilize hydrophobic proteins in the presence of liposomes acting as chaperones
383 [73]. Recently, a phosphocholine based fluorinated derivative (F6OPC) with a perfluorohexyl chain
384 similar to that of FATxPBN was found to partition into POPC bilayers without inducing the solubilization
385 of preformed vesicles [74]. Conversely, Frotscher and co-workers observed the complete solubilization
386 of lipid vesicles after incubation with a fluorinated surfactant bearing the same perfluorohexyl chain
387 and a maltoside polar head group (F6OM) [75]. Our assays did not reveal any significant modification

of the permeability of the membrane, indicating that the fluorinated antioxidants tested here did not solubilize the membrane at the concentration they are the most effective. This is very likely due to the very low concentration (physiologically more relevant) used in the present study (5 % mol, *i.e.* 0.5 µM) compared to the 2 mM used by Frotscher and co-workers.

3.4. MD simulations to support positioning of the fluorinated antioxidants in DLiPC membranes

Each derivative was placed at different positions at the beginning of the MD simulations. It is worth noting that all simulations, each molecule reached similar equilibrium position in the membrane. In other words, when starting from the bulk water all the compounds inserted into the DLiPC lipid bilayers. The preferred (equilibrium) position of the center of mass (COM) of Trolox and PBN were just below the polar head group region in close contact with the phosphates and to a less extent with the choline moieties (14.0 and 13.6 Å for both compounds, respectively from the middle of the bilayer, see Table 2 and Fig. S6 for the radial distribution function). The fluorinated antioxidants also partition just below the polar head group region, the COM being at 14.3, 14.7 and 13.7 Å from the middle of the bilayer for FATx, FAPBN and FATxPBN, respectively (Table 2). The different equilibrium positions obtained from the MD simulations were fully consistent with the chemical structures of these amphiphilic derivatives, as the different moieties drive the preferred location. Namely, from one side, both β-D-Galactose and gluconic acid moieties strongly anchor the derivatives to the choline and to the phosphate groups (*ca*. 16.5 and 20.0 Å for both moieties, respectively, from the middle of the bilayer) by electrostatic and H-bonding interactions (Fig. 6). From another side, the fluorinated chain lines up along the DLiPC lipid chains (COM of the fluorinated chain ranging from 8.2 to 10.4 Å, see Table 2), anchoring the derivatives into the membrane (Fig. 6). In the case of the fluorinated antioxidants, the Trolox and PBN moieties fluctuate below the polar head group region (ranging from 13.8 to 15.7 Å from the middle of the bilayer, see Table 2) with a preferred orientation parallel to the surface (Fig. S7) in close contact with the phosphates, as for the parent Trolox and PBN derivatives.

Interestingly, in the case of FAPBN, the MD simulations, which were performed to ensure a sufficient conformational sampling, highlighted the existence of a second (minor) conformer inside the membrane. In this conformer, the PBN moiety was driven deeper in the membrane (9.0 Å from the middle of the bilayer, see Table 2), in close contact with the fluorinated chain (Fig. 6D). This minor conformer corresponds to a 3-dimensional molecular arrangement which has been observed during short-lasting period along the MD simulation time. In this conformer, PBN is lining up along the fluorinated chain (Fig. 6D), whereas in the major conformer (seen during long-lasting period of the MD simulations), PBN is far apart from the fluorinated chain. Conversely, no similar alignment of the Trolox moiety and the fluorinated chain (in FATx and FATxPBN) was observed throughout the whole MD simulations, even though some initial geometries were driven to put these two moieties were in close contact. As a consequence, no intramolecular interactions between the Trolox and PBN moieties were observed in FATxPBN throughout the whole MD simulations.

4. Discussion

The antioxidant assays conducted in this work highlight that the three fluorinated antioxidants are much more efficient than the parent compounds PBN and Trolox. This is consistent with various other studies on hybrid antioxidants, which showed how the chemical combination of two antioxidant moieties enhances the activity with respect to both moieties taken separately [26–28]. Along the same line to maximize lipid peroxidation activity, we previously conducted a similar study by combining PBN and cholesterol within amphiphilic derivatives [76]. By using similar experimental setups than in the present study, we showed these cholesteryl-PBN derivatives displayed enhanced hydrophobic and antioxidant properties in comparison to the parent compound PBN, as dynamic light scattering and oxidative stress experiments evidenced a stronger ability of cholesteryl-PBNs to stabilize the structure of the vesicles and to preserve them from the swelling due to the oxidation process. The molecules tested in this work, in particular FATxPBN and FATx, present lower IC_{50} values than the cholesteryl-

PBNs, which underline a stronger ability to prevent lipid oxidation, as expected due to the presence of the Trolox moiety.

We observed significant discrepancies between the fluorinated antioxidants, as both FATxPBN and FATx exhibited IC_{50} values that are 49 and 33 times lower (higher activity) than FAPBN, respectively (see Fig. 2). The differences observed between FAPBN and the other two fluorinated antioxidants can be rationalized by a lower affinity to lipid (slightly lower hydrophobicity, see log*P* on Fig. 1) of the former parent compound (*i.e.* PBN) and by the absence of the Trolox moiety in this derivative. The scavenging mechanisms of both Trolox and PBN are different (most probably hydrogen atom abstraction and adduct formation – spin trap –, respectively), which makes the former derivative a much better free radical scavenger. Concomitantly, the amphiphilic feature of the derivatives finely tunes the capacity for lipid peroxidation inhibition, by ensuring a positioning in the membrane below the polar head groups, in close contact with the oxidation process (*i.e.*, as close as possible from unsaturation). At this preferred location, the derivatives are likely to inhibit both the initiation stage or the propagation stage for lipid chains which can adopt a transient snorkel-like shape [77,78] of lipid peroxidation. Also, it is well-known that location of the antioxidants in close contact to the unsaturations of the phospholipid acyl chains favors a better inhibition of lipid peroxidation [79]. The log*P* values suggest that the higher the hydrophobicity, the higher the maximal insertion pressure and the deeper the molecules penetrate into the membrane (Fig. S5 A-B). In accordance with our observations, Azouzi and co-workers recently reported that serotonin has the ability to bind and protect DLiPC enriched membranes from oxidation [80], due to frequent interactions between serotonin and phospholipid acyl chains, which might inhibit the propagation stage of lipid peroxidation.

Interestingly, PBN exhibited no lipid peroxidation inhibition whereas an IC_{50} was measured with FAPBN. As seen from the MD simulations and highly expected from their chemical nature, both PBN itself and the PBN moiety in the major conformer of FAPBN lie at almost the same preferred position.

Therefore, a highly plausible explanation of the better activity of FAPBN with respect to PBN is assigned to an anchoring effect, which is attributed to the fluorinated chain which better constrain (anchor) the positioning of the PBN moiety in the membrane for FAPBN. This can in turn makes the PBN moiety more efficient as a spin trapper. Although hardly directly reachable by experimental techniques, the explanation of the measurable IC_{50} value for FAPBN is likely due to its amphiphilic chemical nature, which allows this anchoring effect in close contact to the region where lipid oxidation occurs. A secondary explanation might be due to the existence of the second (minor) FAPBN conformer (Fig. 7D), in which the PBN moiety may even spend some time deeper in the bilayer to inhibit lipid peroxidation more efficiently than PBN alone, however not as efficient as both FATxPBN and FATx due to a much less efficient free radical scavenging capacity.

FATx is 33 times more active than FAPBN, which is mainly attributed to the nature of the antioxidant moiety and not to positioning. Indeed, Trolox is a much more efficient free radical scavenger than PBN, while the MD simulations suggest that both moieties are positioned in the same membrane region, in close contact with the polar head group region due to their relatively hydrophilic and H-bonding donor/acceptor nature. With an IC_{50} of 0.6 µM, FATxPBN has shown the highest antioxidant activity among all three fluorinated antioxidants. Since FATxPBN presents an IC_{50} lower than the average of FATx and FAPBN, the combination of Trolox and PBN moieties on a same carrier was hypothesized to have created a synergistic antioxidant effect. To confirm or infirm this hypothesis, the activity of FATx and FAPBN was more thoroughly compared to that of FATxPBN to decipher whether the combination result in simple additive, supra-additive (synergistic) or infra-additive (inhibition of one agent by the other) effects. Both FATx and FAPBN are considered here as two separated antioxidant agents engaged in a similar skeleton; *i.e.*, an antioxidant moiety linked to a perfluorinated chain and a sugar moiety. To address this issue, the combination index (CI) of FATx and FAPBN was determined based on the Chou and Talalay method [81]. As one can see in Table 3, at low concentrations (*i.e.*, 0.4 to 0.8 µM) the combination of FATx and FAPBN creates a synergistic

antioxidant effect as CI values are lower than 1. This effect disappears when the concentrations are increased as with concentrations ranging from 1.6 to 38.4 µM, the CI values are higher than 1, suggesting an infra-additive effect (*i.e.* inhibition between both antioxidant moieties). The statistical analysis evidenced significant differences ($p < 0.05$) between the CI values of the low (0.4 to 0.8 µM) and the high concentrations (1.6 to 38.4 µM), which underlines the presence of a synergistic effect at low concentrations. Similar trends (Table. S1) were observed by multiplying the percentages of lipid oxidation of FATx and FAPBN and comparing them to those of FATxPBN according to the Berenbaum method [82,83], leading to similar conclusions.

Several researchers have reported on synergistic effects created by combining different antioxidant moieties. For instance, it has been reported that the combination of β-carotene and α-tocopherol results in a better protection of rat liver microsomes from oxidative stress [84]. Recently, Trolox has been mixed with caffeic acid phenethyl ester (CAPE) to create a synergistic antioxidant effect [85], which was attributed to weak interactions (hydrogen bonds) between Trolox and CAPE. Trolox has also been combined to nitrones to create nitrone derivatives of Trolox [86], which revealed more efficient *in vitro* and *in vivo* activities against lipid peroxidation and ischemia with respect to the parent compounds. Synergism between antioxidants can proceed through different mechanisms like sacrificial oxidation [87], regeneration or other mechanisms [88]. In the case of sacrificial oxidation, one antioxidant protects the other by free radical scavenging, while for regeneration, one antioxidant is oxidized to renew the second one. An extensively-described and typical example of regeneration is the interaction between vitamin E and vitamin C [89]. Other researchers attempted to combine, in a single molecule, different types of antioxidants to favor synergistic effects. For instance, lipoic acid has been combined to Trolox [26] as well as a nitric oxide synthase inhibitor [28] with the objective to obtain greater protective effects. Preliminary experiments on biological systems highlighted that these divalent antioxidants have better abilities to prevent neuronal damage caused by glutamate and oxidation of rat microsomal membrane lipids. Recently, Vavrilokova and co-workers, through

enzymatic reactions, combined silybin to ascorbic acid, Trolox alcohol or tyrosol to obtain novel divalent antioxidants [27]. Among all the derivatives, the derivative combining silybin to ascorbic acid showed the highest ability to protect rat microsomes from lipid peroxidation. Durand and co-workers previously reported the synthesis of PBNLP, a divalent antioxidant bearing a PBN and a lipoic acid moiety [90]. No synergistic antioxidant effect was observed as PBNLP and its individual constituents showed a similar ability to protect red blood cells from AAPH-induced hemolysis. However, the combination of the two moieties on the same carrier strongly diminished the antagonist effect observed between the individual derivatives.

In the case of FATxPBN, no intramolecular interactions between both antioxidant (Trolox and PBN) moieties were observed by MD simulations, which is fully consistent with the amphiphilic nature of the molecule and the chemical nature of the different moieties. This precludes regeneration effect within the same molecule. However, the compounds are likely to accumulate in a narrow region and regarding the similar depth of insertion of both Trolox and PBN moieties, intermolecular interactions are likely to occur. This could favor a regeneration process. This appears possible at relatively low concentration, *i.e.*, below 0.8 µM, as seen by the experimental results. This may correspond to greater local concentration due to partitioning in membrane. In this case small non-covalent clusters can be formed. At higher concentration values this effect disappears (Table 3), most probably due to the formation of higher-order aggregates, in which less antioxidant moieties are available. Also, the ability of FATxPBN to strongly delay lipid oxidation compared to the other antioxidants (see Fig. 3) suggests that this derivative combines the retarding effect of PBN [91] with the free radical scavenging capacity of Trolox [92], thus creating a synergistic effect by retardation. At first, the PBN moiety seems to delay the oxidation during 60 min, as percentages of oxidation of the SUVs are the same, regardless of the concentration of FATxPBN (see Fig. 2A). Then, the dose-dependent antioxidant efficiency observed might be attributed to the Trolox moiety, as FAPBN is only slightly efficient against AAPH-induced oxidation (see Fig. 2F).

538

5. Conclusion

The present work is in line with the strategy aiming at grafting two antioxidant moieties on the same carrier to enhance the global antioxidant action with a nanoscale fine tuning. The key role of the amphiphilic feature of this series of fluorinated antioxidants bearing Trolox and/or PBN moieties was studied in terms of interaction with membranes. The presence of the perfluorinated chain increases hydrophobicity, allowing these derivatives to form monolayers at the air-water interface. Because of higher hydrophobicity, they are anchored to the DLiPC membranes, with a greater antioxidant activity against AAPH-induced lipid oxidation. Interestingly, although PBN is inefficient, its combination with a Trolox moiety on the same carrier creates a synergistic effect that improves the global antioxidant efficiency. Thanks to a dual mode of action, such hybrid antioxidants are very promising molecules for a wide range of applications in cosmetic, food and pharmaceutical industries by lowering the usual concentrations of antioxidant required to efficiently prevent lipid oxidation.

Author's contributions

G.D and S.M conceived this research. M.R synthesized the fluorinated antioxidants. L.S and A.M.G.G performed the experiments with model membranes. B.C and F.D.M designed and performed MD simulations. B.C, F.D.M and P.T analyzed the theoretical data. L.S analyzed the experimental data and wrote the article. P.T, G.D and S.M formatted the manuscript.

Acknowledgements

L. Socrier was the recipient of a PhD scholarship from the French "Ministère de l'enseignement supérieur de la recherche et de l'innovation". Dr M. Rosselin was the recipient of a fellowship from the "Provence Alpes Côte d'Azur" regional council. The "Centre national de la recherche scientifique (CNRS)", the "Université de Technologie de Compiègne" and the "Université d'Avignon et des Pays du Vaucluse" are gratefully acknowledged for providing facilities and financial support. P. Trouillas, B. Chantemargue and F. Di Meo thank CALI, "Nouvelle Aquitaine" regional council and the "Institut national de la santé et de la recherche médicale (INSERM)". P. Trouillas thanks the Czech Science Foundation (P208/12/G016) and the National Program of Sustainability from the Ministry of Youth, Education and Sports of the Czech Republic (LO1305).

Conflict of interest

The authors declare no conflict of interest.

Supporting material

Supporting material (7 figures and 1 table) can be found at

6. References

[1] K. Apel, H. Hirt, Reactive oxygen species: metabolism, oxidative stress, and signal transduction., Annu. Rev. Plant Biol. 55 (2004) 373–99. doi:10.1146/annurev.arplant.55.031903.141701.

[2] H.J. Forman, M. Torres, Reactive oxygen species and cell signaling: respiratory burst in macrophage signaling., Am. J. Respir. Crit. Care Med. 166 (2002) S4-8. doi:10.1164/rccm.2206007.

[3] W. Dröge, Free Radicals in the Physiological Control of Cell Function, Physiol. Rev. 82 (2002) 47–95. doi:10.1152/physrev.00018.2001.

[4] J. Pincemail, M. Meurisse, R. Limet, J.O. Defraigne, Espèces oxygénées activées, antioxydants et cancer, Vaiss. Coeur, Poumons. 4 (1999) 2–5. http://www.vcp-bhl.be/fr/home?tk_id=nosign.

[5] R. Wheatley, Some recent trends in the analytical chemistry of lipid peroxidation, TrAC Trends Anal. Chem. 19 (2000) 617–628. doi:10.1016/S0165-9936(00)00010-8.

[6] R. Sultana, M. Perluigi, D.A. Butterfield, Lipid peroxidation triggers neurodegeneration: A redox proteomics view into the Alzheimer disease brain, Free Radic. Biol. Med. 62 (2013) 157–169. doi:10.1016/j.freeradbiomed.2012.09.027.

[7] G. Kojda, Interactions between NO and reactive oxygen species: pathophysiological importance in atherosclerosis, hypertension, diabetes and heart failure, Cardiovasc. Res. 43 (1999) 562–571. doi:10.1016/S0008-6363(99)00169-8.

[8] G. Waris, H. Ahsan, Reactive oxygen species role in the development of cancer and various chronic conditions, J. Carcinog. 5 (2006) 14. doi:10.1186/1477-3163-5-14.

[9] J. Pardeike, A. Hommoss, R.H. Müller, Lipid nanoparticles (SLN, NLC) in cosmetic and pharmaceutical dermal products, Int. J. Pharm. 366 (2009) 170–184. doi:10.1016/j.ijpharm.2008.10.003.

[10] A.V.S. Perumalla, N.S. Hettiarachchy, Green tea and grape seed extracts — Potential applications in food safety and quality, Food Res. Int. 44 (2011) 827–839. doi:10.1016/j.foodres.2011.01.022.

[11] J. Fernández, J.A. Pérez-Álvarez, J.A. Fernández-López, Thiobarbituric acid test for monitoring lipid oxidation in meat, Food Chem. 59 (1997) 345–353. doi:10.1016/S0308-8146(96)00114-8.

[12] R. Khanum, H. Thevanayagam, Lipid peroxidation: Its effects on the formulation and use of pharmaceutical emulsions, Asian J. Pharm. Sci. 12 (2017) 401–411. doi:10.1016/j.ajps.2017.05.003.

[13] A.M. Pisoschi, A. Pop, The role of antioxidants in the chemistry of oxidative stress: A review, Eur. J. Med. Chem. 97 (2015) 55–74. doi:10.1016/j.ejmech.2015.04.040.

[14] V.J. Forrest, Y.-H. Kang, D.E. McClain, D.H. Robinson, N. Ramakrishnan, Oxidative stress-induced apoptosis prevented by trolox, Free Radic. Biol. Med. 16 (1994) 675–684. doi:10.1016/0891-5849(94)90182-1.

[15] V.F. Sagach, M. Scrosati, J. Fielding, G. Rossoni, C. Galli, F. Visioli, The water-soluble vitamin E analogue Trolox protects against ischaemia/reperfusion damage in vitro and ex vivo. A comparison with vitamin E, Pharmacol. Res. 45 (2002) 435–439. doi:10.1006/phrs.2002.0993.

[16] L.R.C. Barclay, M.R. Vinqvist, Membrane peroxidation: Inhibiting effects of water- soluble antioxidants on phospholipids of different charge types, Free Radic. Biol. Med. 16 (1994) 779–788. doi:10.1016/0891-5849(94)90193-7.

[17] N.J. Miller, C. Rice-Evans, M.J. Davies, V. Gopinathan, A. Milner, A Novel Method for Measuring Antioxidant Capacity and its Application to Monitoring the Antioxidant Status in Premature Neonates, Clin. Sci. 84 (1993) 407–412. doi:10.1042/cs0840407.

[18] R. van den Berg, G.R.M.M. Haenen, H. van den Berg, A. Bast, Applicability of an improved Trolox equivalent antioxidant capacity (TEAC) assay for evaluation of antioxidant capacity measurements of mixtures, Food Chem. 66 (1999) 511–517. doi:10.1016/S0308-8146(99)00089-8.

[19] E. Finkelstein, G.M. Rosen, E.J. Rauckman, Spin trapping of superoxide and hydroxyl radical: Practical aspects, Arch. Biochem. Biophys. 200 (1980) 1–16. doi:10.1016/0003-9861(80)90323-9.

[20] R.A. Floyd, K. Hensley, M.J. Forster, J.A. Kelleher-Andersson, P.L. Wood, Nitrones, their value as therapeutics and probes to understand aging, Mech. Ageing Dev. 123 (2002) 1021–1031. doi:10.1016/S0047-6374(01)00385-2.

[21] S. Doblas, D. Saunders, P. Kshirsagar, Q. Pye, J. Oblander, B. Gordon, S. Kosanke, R.A. Floyd, R.A. Towner, Phenyl-tert-butylnitrone induces tumor regression and decreases angiogenesis in a C6 rat glioma model, Free Radic. Biol. Med. 44 (2008) 63–72. doi:10.1016/j.freeradbiomed.2007.09.006.

[22] R.A. Floyd, H.C.C.F. Neto, G.A. Zimmerman, K. Hensley, R.A. Towner, Nitrone-based therapeutics for neurodegenerative diseases: Their use alone or in combination with lanthionines, Free Radic. Biol. Med. 62 (2013) 145–156. doi:10.1016/j.freeradbiomed.2013.01.033.

[23] M.I. Ayuso, M. Chioua, E. Martínez-Alonso, E. Soriano, J. Montaner, J. Masjuán, D.J. Hadjipavlou-Litina, J. Marco-Contelles, A. Alcázar, CholesteroNitrones for Stroke, J. Med. Chem. 58 (2015) 6704–6709. doi:10.1021/acs.jmedchem.5b00755.

[24] F. Choteau, G. Durand, I. Ranchon-Cole, C. Cercy, B. Pucci, Cholesterol-based α-phenyl-N-tert-butyl nitrone derivatives as antioxidants against light-induced retinal degeneration., Bioorg. Med. Chem. Lett. 20 (2010) 7405–9. doi:10.1016/j.bmcl.2010.10.037.

[25] H.Y. Zhang, D.P. Yang, G.Y. Tang, Multipotent antioxidants: from screening to design, Drug Discov. Today. 11 (2006) 749–754. doi:10.1016/j.drudis.2006.06.007.

[26] M. Koufaki, T. Calogeropoulou, A. Detsi, A. Roditis, A.P. Kourounakis, P. Papazafiri, K. Tsiakitzis, C. Gaitanaki, I. Beis, P.N. Kourounakis, Novel potent inhibitors of lipid peroxidation with protective effects against reperfusion arrhythmias, J. Med. Chem. 44 (2001) 4300–4303. doi:10.1021/jm010962w.

[27] E. Vavříková, V. Křen, L. Jezova-Kalachova, M. Biler, B. Chantemargue, M. Pyszková, S. Riva, M. Kuzma, K. Valentová, J. Ulrichová, J. Vrba, P. Trouillas, J. Vacek, Novel flavonolignan hybrid antioxidants: From enzymatic preparation to molecular rationalization, Eur. J. Med. Chem. 127

649 (2017) 263–274. doi:10.1016/j.ejmech.2016.12.051.
650 [28] J.J. Harnett, M. Auguet, I. Viossat, C. Dolo, D. Bigg, P.E. Chabrier, Novel lipoic acid analogues that
651 inhibit nitric oxide synthase, Bioorg. Med. Chem. Lett. 12 (2002) 1439–1442. doi:Pii S0960-
652 894x(02)00216-0\rDoi 10.1016/S0960-894x(02)00216-0.
653 [29] S. Ortial, G. Durand, B. Poeggeler, A. Polidori, M.A. Pappolla, J. Böker, R. Hardeland, B. Pucci,
654 Fluorinated amphiphilic amino acid derivatives as antioxidant carriers: A new class of protective
655 agents, J. Med. Chem. 49 (2006) 2812–2820. doi:10.1021/jm060027e.
656 [30] M. Rosselin, G. Meyer, P. Guillet, T. Cheviet, G. Walther, A. Meister, D. Hadjipavlou-Litina, G.
657 Durand, Divalent Amino-Acid-Based Amphiphilic Antioxidants: Synthesis, Self-Assembling
658 Properties, and Biological Evaluation, Bioconjug. Chem. 27 (2016) 772–781.
659 doi:10.1021/acs.bioconjchem.6b00002.
660 [31] C. Der Mardirossian, M.P. Krafft, T. Gulik-Krzywicki, M. Le Maire, F. Lederer,
661 Perfluoroalkylphosphocholines are poor protein-solubilizing surfactants, as tested with
662 neutrophil plasma membranes, Biochimie. 80 (1998) 531–541. doi:10.1016/S0300-
663 9084(00)80018-8.
664 [32] S.-W. Huang, E.N. Frankel, Antioxidant Activity of Tea Catechins in Different Lipid Systems, J.
665 Agric. Food Chem. 45 (1997) 3033–3038. doi:10.1021/jf9609744.
666 [33] V. Kristinová, R. Mozuraityte, I. Storrø, T. Rustad, Antioxidant activity of phenolic acids in lipid
667 oxidation catalyzed by different prooxidants, J. Agric. Food Chem. 57 (2009) 10377–10385.
668 doi:10.1021/jf901072t.
669 [34] E. Niki, Free radical initiators as source of water- or lipid-soluble peroxyl radicals., Methods
670 Enzymol. 186 (1990) 100–8. doi:10.1016/0076-6879(90)86095-D.
671 [35] J. Werber, Y.J. Wang, M. Milligan, X. Li, J.A. Ji, Analysis of 2,2'-Azobis (2-amidinopropane)
672 dihydrochloride degradation and hydrolysis in aqueous solutions, J. Pharm. Sci. 100 (2011)
673 3307–3315. doi:10.1002/jps.22578.

[36] R.O. Recknagel, E.A. Glende, [40] Spectrophotometric Detection of Lipid Conjugated Dienes, Methods Enzymol. (1984). doi:10.1016/S0076-6879(84)05043-6.

[37] E. Schnitzer, I. Pinchuk, D. Lichtenberg, Peroxidation of liposomal lipids, Eur. Biophys. J. 36 (2007) 499–515. doi:10.1007/s00249-007-0146-2.

[38] J.F.D. Liljeblad, V. Bulone, E. Tyrode, M.W. Rutland, C.M. Johnson, Phospholipid monolayers probed by vibrational sum frequency spectroscopy: Instability of unsaturated phospholipids, Biophys. J. 98 (2010) L50–L52. doi:10.1016/j.bpj.2010.02.009.

[39] E. Tyrode, P. Niga, M. Johnson, M.W. Rutland, Molecular structure upon compression and stability toward oxidation of langmuir films of unsaturated fatty acids: A vibrational sum frequency spectroscopy study, Langmuir. 26 (2010) 14024–14031. doi:10.1021/la102189z.

[40] P. Calvez, E. Demers, E. Boisselier, C. Salesse, Analysis of the contribution of saturated and polyunsaturated phospholipid monolayers to the binding of proteins, Langmuir. 27 (2011) 1373–1379. doi:10.1021/la104097n.

[41] É. Boisselier, É. Demers, L. Cantin, C. Salesse, How to gather useful and valuable information from protein binding measurements using Langmuir lipid monolayers, Adv. Colloid Interface Sci. 243 (2017) 60–76. doi:10.1016/j.cis.2017.03.004.

[42] P. Suttiprasit, V. Krisdhasima, J. McGuire, The surface activity of α-lactalbumin, β-lactoglobulin, and bovine serum albumin, J. Colloid Interface Sci. 154 (1992) 316–326. doi:10.1016/0021-9797(92)90146-D.

[43] R. Maget-Dana, M. Ptak, Behavior of insect defensin A at the air/water interface, Colloids Surfaces B Biointerfaces. 7 (1996) 135–143. doi:10.1016/0927-7765(96)01292-1.

[44] J.C. Stewart, Colorimetric determination of phospholipids with ammonium ferrothiocyanate., Anal. Biochem. 104 (1980) 10–4. doi:10.1016/0003-2697(80)90269-9.

[45] E.L. Wu, X. Cheng, S. Jo, H. Rui, K.C. Song, E.M. Dávila-Contreras, Y. Qi, J. Lee, V. Monje-Galvan, R.M. Venable, J.B. Klauda, W. Im, CHARMM-GUI membrane builder toward realistic biological

membrane simulations, J. Comput. Chem. 35 (2014) 1997–2004. doi:10.1002/jcc.23702.

[46] Å.A. Skjevik, B.D. Madej, R.C. Walker, K. Teigen, LIPID11: A Modular Framework for Lipid Simulations Using Amber, J. Phys. Chem. B. 116 (2012) 11124–11136. doi:10.1021/jp3059992.

[47] J. Wang, R.M. Wolf, J.W. Caldwell, P.A. Kollman, D.A. Case, Development and testing of a general amber force field, J. Comput. Chem. 25 (2004) 1157–1174. doi:10.1002/jcc.20035.

[48] J. Wang, T. Hou, Application of molecular dynamics simulations in molecular property prediction. 1. Density and heat of vaporization, J. Chem. Theory Comput. 7 (2011) 2151–2165. doi:10.1021/ct200142z.

[49] D.L. Mobley, C.I. Bayly, M.D. Cooper, M.R. Shirts, K.A. Dill, Small molecule hydration free energies in explicit solvent: An extensive test of fixed-charge atomistic simulations, J. Chem. Theory Comput. 5 (2009) 350–358. doi:10.1021/ct800409d.

[50] K.N. Kirschner, A.B. Yongye, S.M. Tschampel, J. González-Outeiriño, C.R. Daniels, B.L. Foley, R.J. Woods, GLYCAM06: A generalizable biomolecular force field. carbohydrates, J. Comput. Chem. 29 (2008) 622–655. doi:10.1002/jcc.20820.

[51] J. Wang, W. Wang, P.A. Kollman, D.A. Case, Automatic atom type and bond type perception in molecular mechanical calculations, J. Mol. Graph. Model. 25 (2006) 247–260. doi:10.1016/j.jmgm.2005.12.005.

[52] Y. Duan, C. Wu, S. Chowdhury, M.C. Lee, G. Xiong, W. Zhang, R. Yang, P. Cieplak, R. Luo, T. Lee, J. Caldwell, J. Wang, P. Kollman, A point-charge force field for molecular mechanics simulations of proteins based on condensed-phase quantum mechanical calculations, J. Comput. Chem. 24 (2003) 1999–2012. doi:10.1002/jcc.10349.

[53] M.J. Frish, G.W. Trucks, H.B. Schlegel, G.E. Scuseria, M.A. Robb, J.R. Cheeseman, G. Scalmani, V. Barone, G.A. Petersson, H. Nakatsuji, X. Li, M. Caricato, A. Marenich, J. Bloino, G. Janesko, R. Gomperts, B. Mennucci, H.P. Hratchian, V. Ortiz, A.F. Izmaylov, J.L. Sonnenberg, D. Williams-Young, F. Ding, F. Lipparini, F. Egidi, J. Goings, B. Peng, A. Petrone, T. Henderson, D. Ranasinghe,

V.G. Zakrzewski, J. Gao, N. Rega, G. Zheng, W. Liang, M. Hada, M. Ehara, K. Toyota, R. Fukuda, J. Hasegawa, M. Ishida, T. Nakajima, Y. Honda, O. Kitao, H. Nakai, T. Vreven, K. Throssel, J.A. Montgomery, J.E. Peralta, F. Ogliaro, M. Bearpark, J.J. Heyd, E. Brothers, K.N. Kudin, V.N. Staroverov, T. Keith, R. Kobayashi, J. Normand, K. Raghavachari, A. Rendell, J.C. Burant, S.S. Iyengar, J. Tomasi, M. Cossi, J.M. Millam, M. Klene, C. Adamo, R. Cammi, J.W. Ochterski, R.L. Martin, K. Morokuma, O. Farkas, J.B. Foresman, D.J. Fox, Gaussian, Inc., Wallingford CT, 2016, n.d.

[54] F.-Y. Dupradeau, A. Pigache, T. Zaffran, C. Savineau, R. Lelong, N. Grivel, D. Lelong, W. Rosanski, P. Cieplak, The R.E.D. Tools: Advances in RESP and ESP charge derivation and force field library building, Phys. Chem. Chem. Phys. 12 (2010) 7821–7839. doi:10.1039/c0cp00111b.

[55] W.L. Jorgensen, J. Chandrasekhar, J.D. Madura, R.W. Impey, M.L. Klein, Comparison of simple potential functions for simulating liquid water, J. Chem. Phys. 79 (1983) 926–935. doi:10.1063/1.445869.

[56] T. Darden, D. York, L. Pedersen, Particle mesh Ewald: An N ·log(N) method for Ewald sums in large systems, J. Chem. Phys. 98 (1993) 10089–10092. doi:10.1063/1.464397.

[57] D.A. Case, D.S. Cerutti, T.E.. Cheatham, T.A. Darden, R.E. Duke, T.J. Giese, H. Gohlke, A.W. Goetz, D. Greene, N. Homeyer, AMBER 2017;University of California: San Francisco, CA, USA, 2017, (n.d.).

[58] R. Salomon-Ferrer, D.A. Case, R.C. Walker, An overview of the Amber biomolecular simulation package, Wiley Interdiscip. Rev. Comput. Mol. Sci. 3 (2013) 198–210. doi:10.1002/wcms.1121.

[59] J.-P. Ryckaert, G. Ciccotti, H.J.C. Berendsen, Numerical integration of the cartesian equations of motion of a system with constraints: molecular dynamics of n-alkanes, J. Comput. Phys. 23 (1977) 327–341. doi:10.1016/0021-9991(77)90098-5.

[60] R.J. Loncharich, B.R. Brooks, R.W. Pastor, Langevin dynamics of peptides: The frictional dependence of isomerization rates of N-acetylalanyl-N'-methylamide, Biopolymers. 32 (1992)

523–535. doi:10.1002/bip.360320508.

[61] H.J.C. Berendsen, J.P.M. Postma, W.F. Van Gunsteren, A. Dinola, J.R. Haak, Molecular dynamics with coupling to an external bath, J. Chem. Phys. 81 (1984) 3684–3690. doi:10.1063/1.448118.

[62] D.R. Roe, T.E. Cheatham, PTRAJ and CPPTRAJ: Software for Processing and Analysis of Molecular Dynamics Trajectory Data, J. Chem. Theory Comput. 9 (2013) 3084–3095. doi:10.1021/ct400341p.

[63] G. Ottaviani, S. Wendelspiess, R. Alvarez-Sánchez, Importance of critical micellar concentration for the prediction of solubility enhancement in biorelevant media, Mol. Pharm. 12 (2015) 1171–1179. doi:10.1021/mp5006992.

[64] D. Marsh, Lateral pressure in membranes, Biochim. Biophys. Acta - Rev. Biomembr. 1286 (1996) 183–223. doi:10.1016/S0304-4157(96)00009-3.

[65] M.P. Krafft, M. Goldmann, Monolayers made from fluorinated amphiphiles, Curr. Opin. Colloid Interface Sci. (2003). doi:10.1016/S1359-0294(03)00046-3.

[66] H. Nakahara, O. Shibata, Langmuir Monolayer Miscibility of Perfluorocarboxylic Acids with Biomembrane Constituents at the Air-Water Interface, J. Oleo Sci. (2012). doi:10.5650/jos.61.197.

[67] N. Funasaki, S. Hada, Coexistence of two kinds of mixed micelles, J. Phys. Chem. 84 (1980) 736–744. doi:10.1021/j100444a010.

[68] V. Peyre, S. Patil, G. Durand, B. Pucci, Mixtures of hydrogenated and fluorinated lactobionamide surfactants with cationic surfactants: Study of hydrogenated and fluorinated chains miscibility through potentiometric techniques, Langmuir. 23 (2007) 11465–11474. doi:10.1021/la701579e.

[69] S. Dong, G. Xu, H. Hoffmann, Aggregation Behavior of Fluorocarbon and Hydrocarbon Cationic Surfactant Mixtures: A Study of 1 H NMR and 19 F NMR, J. Phys. Chem. B. 112 (2008) 9371–9378. doi:10.1021/jp801216e.

[70] P. Barthélémy, V. Tomao, J. Selb, Y. Chaudier, B. Pucci, Fluorocarbon-hydrocarbon nonionic

774 surfactants mixtures: A study of their miscibility, Langmuir. 18 (2002) 2557–2563.
775 doi:10.1021/la011600u.
776 [71] E. Frotscher, J. Höring, G. Durand, C. Vargas, S. Keller, Model-Free Analysis of Critical Micellar
777 Concentrations for Detecting Demixing in Surfactant Mixtures, Anal. Chem. 89 (2017) 3245–
778 3249. doi:10.1021/acs.analchem.7b00339.
779 [72] J.M.C. Gutteridge, B. Halliwell, Antioxidants: Molecules, medicines, and myths, Biochem.
780 Biophys. Res. Commun. 393 (2010) 561–564. doi:10.1016/j.bbrc.2010.02.071.
781 [73] A. Kyrychenko, M. V. Rodnin, M. Vargas-Uribe, S.K. Sharma, G. Durand, B. Pucci, J.L. Popot, A.S.
782 Ladokhin, Folding of diphtheria toxin T-domain in the presence of amphipols and fluorinated
783 surfactants: Toward thermodynamic measurements of membrane protein folding, Biochim.
784 Biophys. Acta - Biomembr. 1818 (2012) 1006–1012. doi:10.1016/j.bbamem.2011.09.012.
785 [74] C. Vargas, R.C. Arenas, E. Frotscher, S. Keller, Nanoparticle self-assembly in mixtures of
786 phospholipids with styrene/maleic acid copolymers or fluorinated surfactants, Nanoscale. 7
787 (2015) 20685–20696. doi:10.1039/c5nr06353a.
788 [75] E. Frotscher, B. Danielczak, C. Vargas, A. Meister, G. Durand, S. Keller, A Fluorinated Detergent
789 for Membrane-Protein Applications, Angew. Chemie Int. Ed. 54 (2015) 5069–5073.
790 doi:10.1002/anie.201412359.
791 [76] L. Socrier, M. Rosselin, F. Choteau, G. Durand, S. Morandat, Cholesterol-nitrone conjugates as
792 protective agents against lipid oxidation: A model membrane study., Biochim. Biophys. Acta.
793 1859 (2017) 2495–2504. doi:10.1016/j.bbamem.2017.09.026.
794 [77] D. Marquardt, J.A. Williams, N. Kučerka, J. Atkinson, S.R. Wassall, J. Katsaras, T.A. Harroun,
795 Tocopherol activity correlates with its location in a membrane: A new perspective on the
796 antioxidant vitamin e, J. Am. Chem. Soc. 135 (2013) 7523–7533. doi:10.1021/ja312665r.
797 [78] J. Garrec, A. Monari, X. Assfeld, L.M. Mir, M. Tarek, Lipid peroxidation in membranes: The
798 peroxyl radical does not “float,” J. Phys. Chem. Lett. 5 (2014) 1653–1658.

799 doi:10.1021/jz500502q.
800 [79] P. Košinová, K. Berka, M. Wykes, M. Otyepka, P. Trouillas, Positioning of Antioxidant Quercetin
801 and Its Metabolites in Lipid Bilayer Membranes: Implication for Their Lipid-Peroxidation
802 Inhibition, J. Phys. Chem. B. 116 (2012) 1309–1318. doi:10.1021/jp208731g.
803 [80] S. Azouzi, H. Santuz, S. Morandat, C. Pereira, F. Côté, O. Hermine, K. El Kirat, Y. Colin, C. Le Van
804 Kim, C. Etchebest, P. Amireault, Antioxidant and Membrane Binding Properties of Serotonin
805 Protect Lipids from Oxidation, Biophys. J. 112 (2017) 1863–1873. doi:10.1016/j.bpj.2017.03.037.
806 [81] T.C. Chou, P. Talalay, Quantitative analysis of dose-effect relationships: the combined effects of
807 multiple drugs or enzyme inhibitors, Adv. Enzyme Regul. 22 (1984) 27–55. doi:10.1016/0065-
808 2571(84)90007-4.
809 [82] M.C. Berenbaum, Criteria for analyzing interactions between biologically active agents, Adv.
810 Cancer Res. 35 (1981) 269–335. doi:10.1016/S0065-230X(08)60912-4.
811 [83] C. Hennequin, N. Giocanti, V. Favaudon, Interaction of ionizing radiation with paclitaxel (taxol)
812 and docetaxel (taxotere) in HeLa and SQ20B cells, Cancer Res. 56 (1996) 1842–1850.
813 [84] P. Palozza, N.I. Krinsky, Beta-Carotene and alpha-tocopherol are synergistic antioxidants, Arch.
814 Biochem. Biophys. 297 (1992) 184–187. doi:10.1016/0003-9861(92)90658-J.
815 [85] H. Bai, R. Liu, H.L. Chen, W. Zhang, X. Wang, X. Di Zhang, W.L. Li, C.X. Hai, Enhanced antioxidant
816 effect of caffeic acid phenethyl ester and Trolox in combination against radiation induced-
817 oxidative stress, Chem. Biol. Interact. 207 (2014) 7–15. doi:10.1016/j.cbi.2013.10.022.
818 [86] G.T. Balogh, K. Vukics, Á. Könczöl, Á. Kis-Varga, A. Gere, J. Fischer, Nitrone derivatives of trolox
819 as neuroprotective agents, Bioorg. Med. Chem. Lett. 15 (2005) 3012–3015.
820 doi:10.1016/j.bmcl.2005.04.043.
821 [87] G. Neunert, P. Górnaś, K. Dwiecki, A. Siger, K. Polewski, Synergistic and antagonistic effects
822 between alpha-tocopherol and phenolic acids in liposome system: spectroscopic study, Eur.
823 Food Res. Technol. 241 (2015) 749–757. doi:10.1007/s00217-015-2500-4.

[88] E.M. Becker, L.R. Nissen, L.H. Skibsted, Antioxidant evaluation protocols: Food quality or health effects, Eur. Food Res. Technol. 219 (2004) 561–571. doi:10.1007/s00217-004-1012-4.

[89] A. Kamal-Eldin, L.-Å. Appelqvist, The chemistry and antioxidant properties of tocopherols and tocotrienols, Lipids. 31 (1996) 671–701. doi:10.1007/BF02522884.

[90] G. Durand, A. Polidori, J.P. Salles, M. Prost, P. Durand, B. Pucci, Synthesis and antioxidant efficiency of a new amphiphilic spin-trap derived from PBN and lipoic acid, Bioorganic Med. Chem. Lett. 13 (2003) 2673–2676. doi:10.1016/S0960-894X(03)00545-6.

[91] L.R.C. Barclay, M.R. Vinqvist, Do spin traps also act as classical chain-breaking antioxidants? A quantitative kinetic study of phenyl tert-butylnitrone (PBN) in solution and in liposomes, Free Radic. Biol. Med. 28 (2000) 1079–1090. doi:10.1016/S0891-5849(00)00197-0.

[92] F. Franzoni, R. Colognato, F. Galetta, I. Laurenza, M. Barsotti, R. Di Stefano, R. Bocchetti, F. Regoli, A. Carpi, A. Balbarini, L. Migliore, G. Santoro, An in vitro study on the free radical scavenging capacity of ergothioneine: comparison with reduced glutathione, uric acid and trolox, Biomed. Pharmacother. 60 (2006) 453–457. doi:10.1016/j.biopha.2006.07.015.

840 **Figure's captions**

841 Fig. 1. Chemical structures and log*P* values of the studied molecules.

842

843 Fig. 2. Effect of the parent compounds and the fluorinated derivatives on the AAPH-induced oxidation
844 of DLiPC SUVs. Kinetics of oxidation in presence of FATxPBN (A). IC_{50} (μM) of Trolox (B), PBN (C), FATx
845 (D), FAPBN (E) and FATxPBN (F). Results are presented as the mean ± standard deviation of at least
846 three independent experiments.

847

848 Fig. 3. Lag time necessary to reach 10 and 20 % of oxidation. Results are presented as the mean ±
849 standard deviation of at least three independent experiments.

850

851 Fig. 4. Surface activity (Gibbs monolayers) of the fluorinated antioxidants at the air/water interface.
852 FATxPBN (A), FATx (B) and FAPBN (C). Data were fitted with a Langmuir equation with GraphPadPrism
853 software.

854

855 Fig. 5. Interactions of fluorinated antioxidants with DLiPC monolayers. FATxPBN (A), FATx (B), FAPBN
856 (C).

857

858 Fig. 6. Kinetics of penetration of the fluorinated antioxidants in DLiPC monolayers at 30 mN/m, which is
859 the lateral pressure of biological membranes [64]. Evolution of the monolayer pressure after the
860 injection of FAPBN, FATx and FATxPBN in DLiPC monolayers at 30 mN/m (A). Determination of the rate
861 coefficient (*k*) after injection of the fluorinated antioxidants in the subphase of DLiPC monolayers (B).

862

863 Fig. 7. Representative snapshots of the preferred location of FATx (A), FAPBN (B) and FATxPBN (C). Fig.
864 6D depicts the minor conformation of FAPBN, in which the PBN moiety is lined up along the fluorinated
865 chain. The 1LB (β-D-Galactose), GA4 (gluconic acid), DAH (2,6-diaminohexanoic acid) and DFA
866 (3,3,4,4,5,5,6,6,7,7,8,8,8-dodecafluorooctan-1-amine) moieties are depicted in red, blue, brown and
867 yellow, respectively. Trolox and PBN are depicted in grey and pink, respectively. The cholines are
868 depicted in cyan, the phosphates are depicted in magenta, 1^{st} and 2^{nd} unsaturations are depicted in
869 green and dark-green, respectively.

Table's captions

Table 1. Binding parameters and rate of penetration (*k*) of the fluorinated antioxidants in DLiPC monolayers.

Table 2. Positions given as distances from the middle of the bilayer (in Å) of key moieties of DLiPC (*i.e.,* choline, phosphates, unsaturations) and the different derivatives Trolox, Anionic Trolox, PBN, FATx, FAPBN, minor conformer of FAPBN (FAPBN*) and FATxPBN (*i.e.,* Trolox moiety, Trolox OH-phenolic, PBN, PBN amine moiety, 1LB = β-D-Galactose, GA4 = gluconic acid; DAH = 2,6-diaminohexanoic acid, DFA = 3,3,4,4,5,5,6,6,7,7,8,8,8-dodecafluorooctan-1-amine), as well as center-of-mass (COM) of the three fluorinated antioxidants FATx, FAPBN and FATxPBN. The positions were averaged over the second half of the MD simulations.

Table 3. Combination index (CI) of FATx and FAPBN. CI<1: supra-additive, CI=1: additive, CI>1: infra-additive. Values with different superscripts differ significantly ($p < 0.05$).

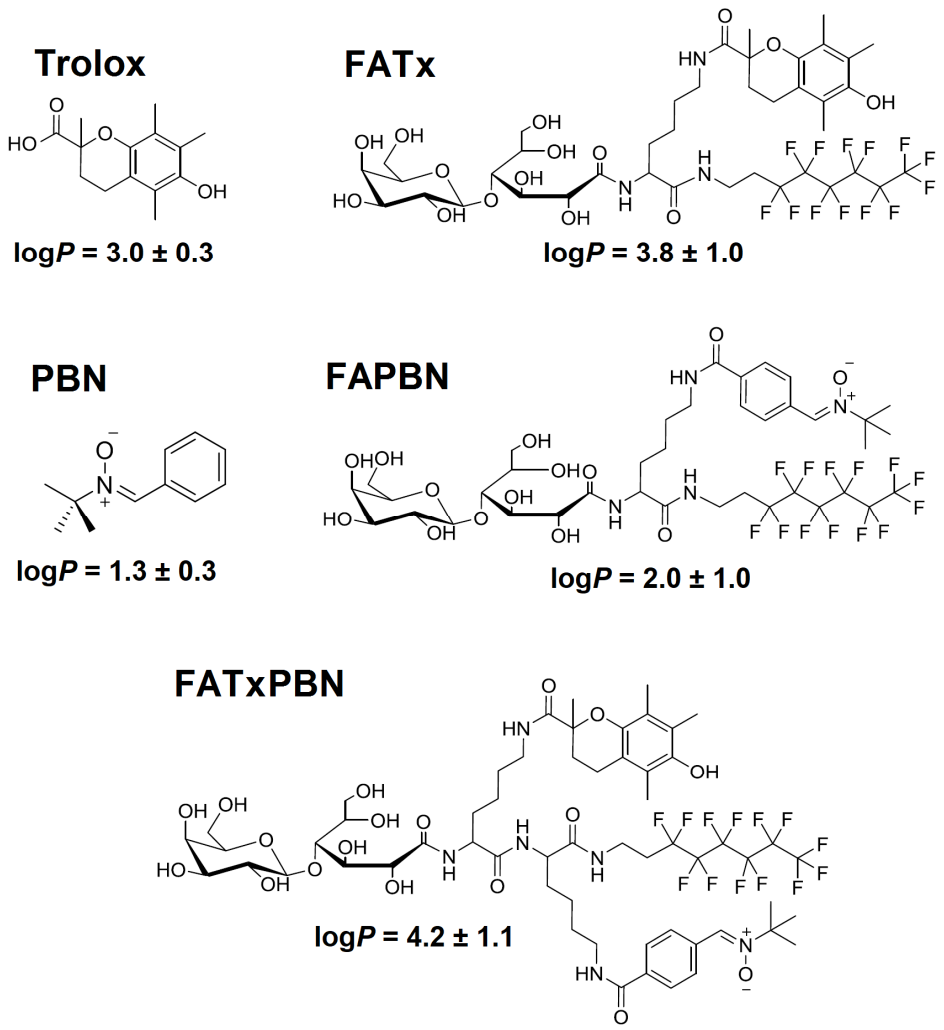

Fig. 1. Chemical structures and log*P* values of the studied molecules.

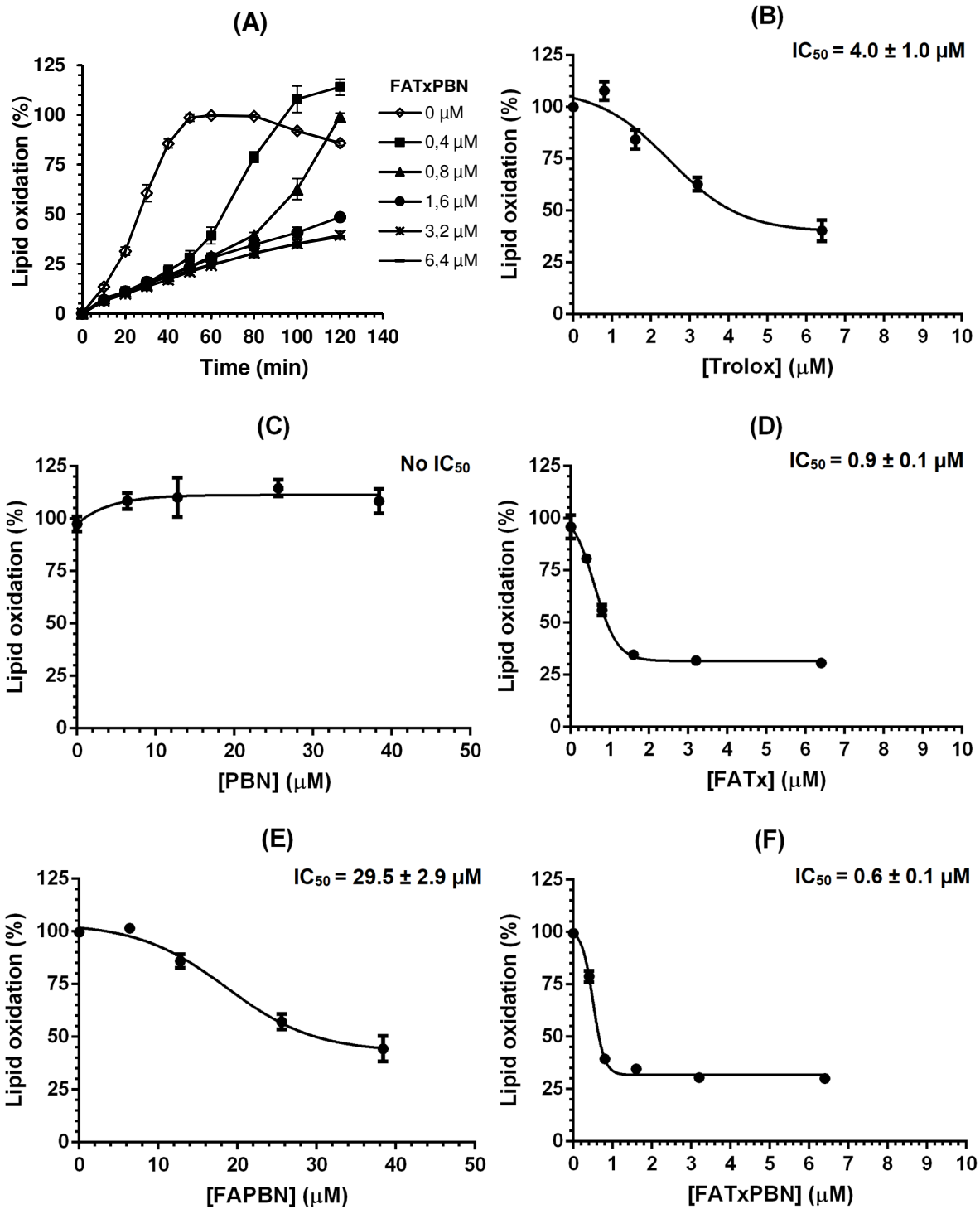

Fig. 2. Effect of the parent compounds and the fluorinated derivatives on the AAPH-induced oxidation of DLPC liposomes. Kinetics of oxidation in presence of FATxPBN (A). IC_{50} (µM) of Trolox (B), PBN (C), FATx (D), FAPBN (E) and FATxPBN (F). Results are presented as the mean ± standard deviation of at least three independent experiments.

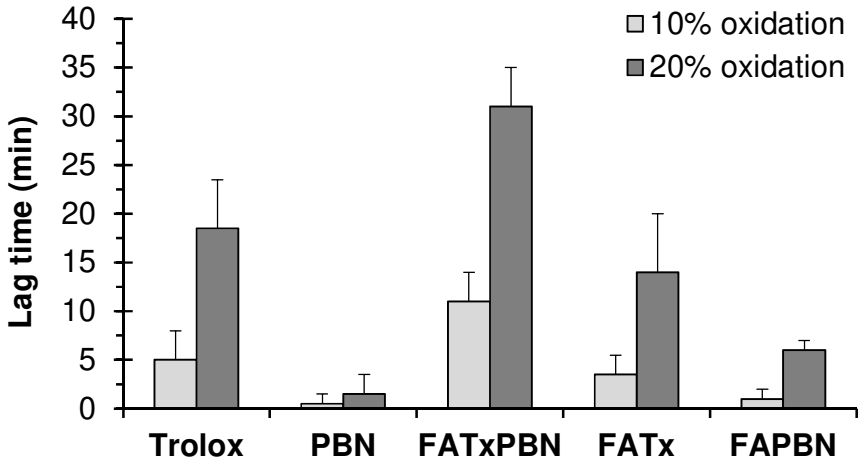

Fig. 3. Lag time necessary to reach 10 and 20 % of oxidation. Results are presented as the mean ± standard deviation of at least three independent experiments.

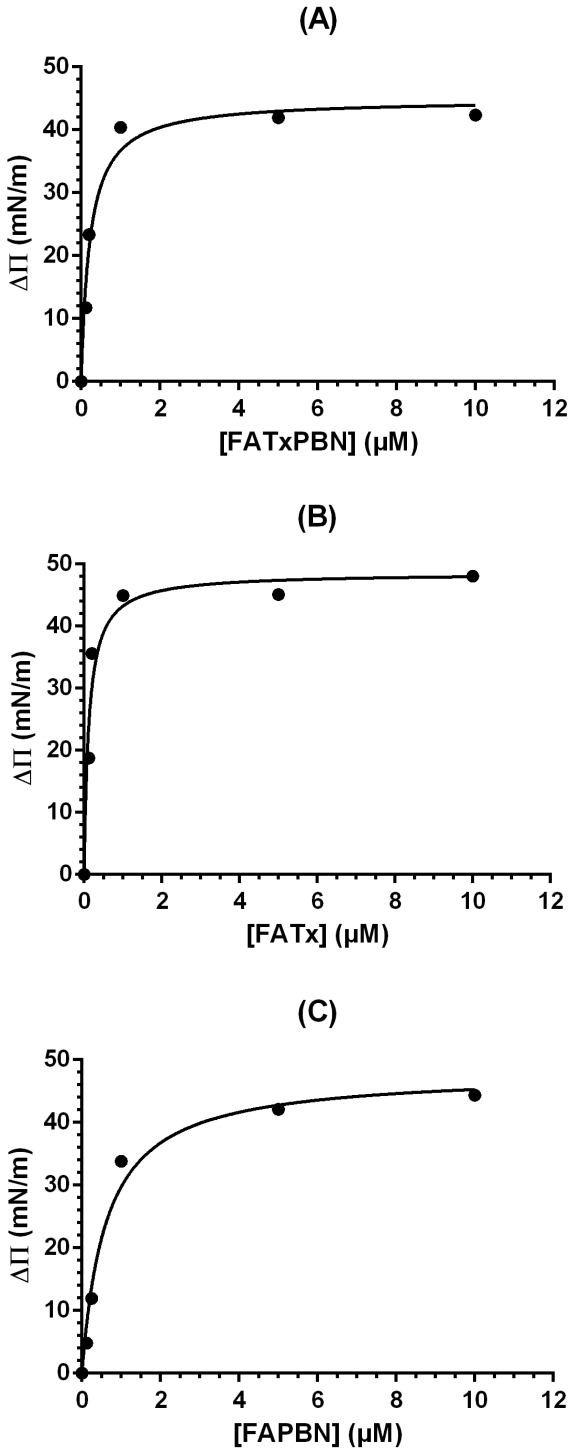

Fig. 4. Surface activity (Gibbs monolayers) of the fluorinated antioxidants at the air/water interface. FATxPBN (A), FATx (B) and FAPBN (C). Each experimental point was performed one time, as described in [40]. Data were fitted with a Langmuir equation with GraphPadPrism software.

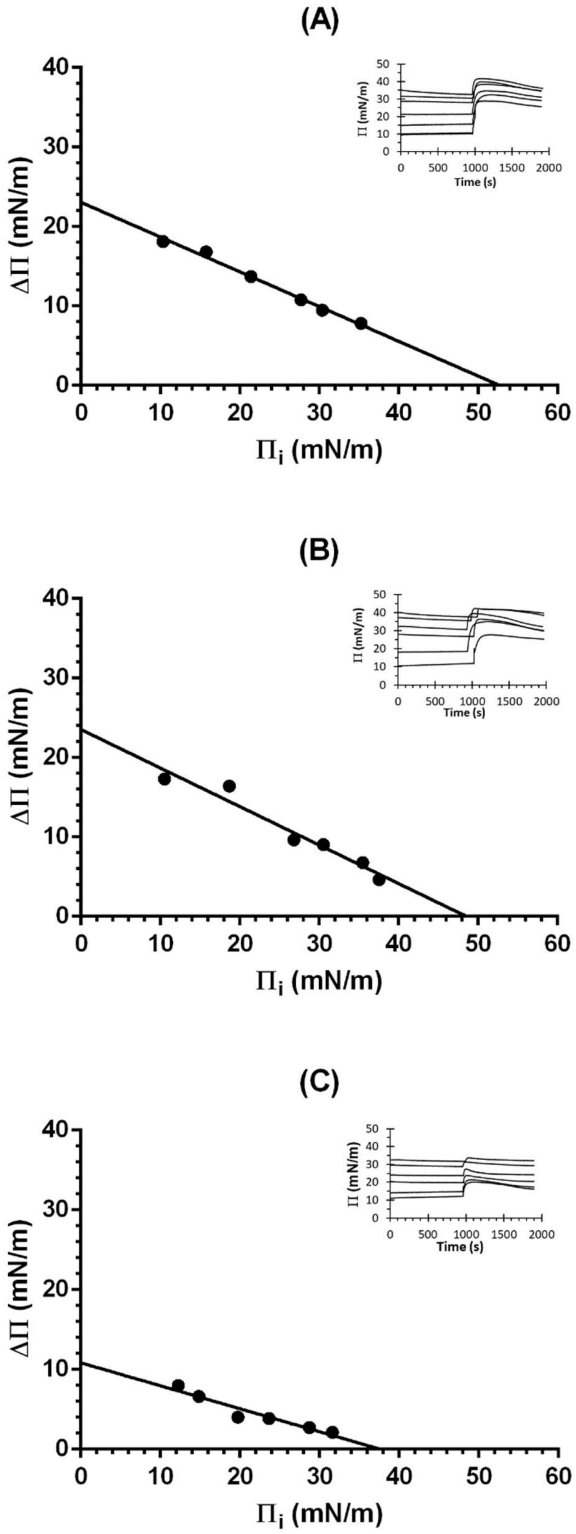

Fig. 5. Interactions of fluorinated antioxidants with DLPC monolayers. FATxPBN (A), FATx (B), FAPBN (C). Upper right boxes: Kinetics of insertion of antioxidants at different surface pressures. Each experimental point was performed one time, as described in [40].

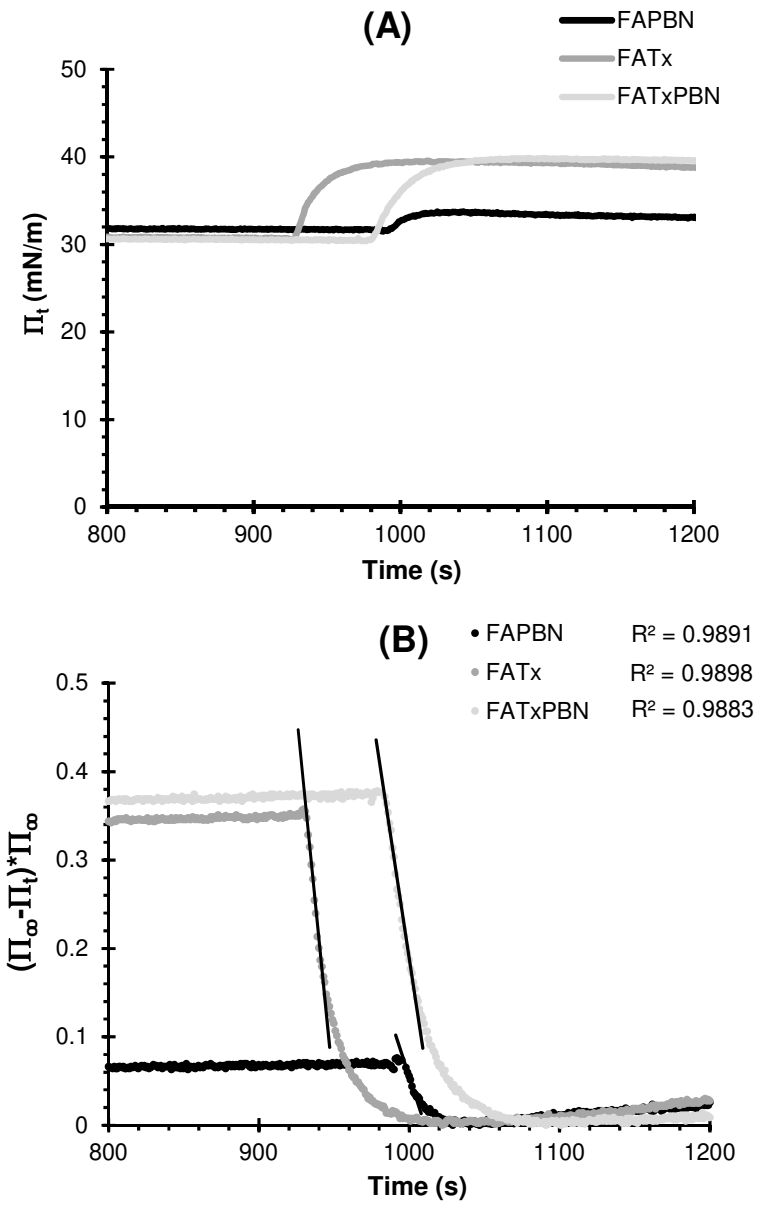

Fig. 6 Kinetics of penetration of the fluorinated antioxidants in DLiPC monolayers at 30 mN/m, which is the lateral pressure of biological membranes [64]. Evolution of the monolayer pressure after the injection of FAPBN, FATx and FATxPBN in DLiPC monolayers at 30 mN/m (A). Determination of the rate coefficient (*k*) after injection of the fluorinated antioxidants in the subphase of DLiPC monolayers (B).

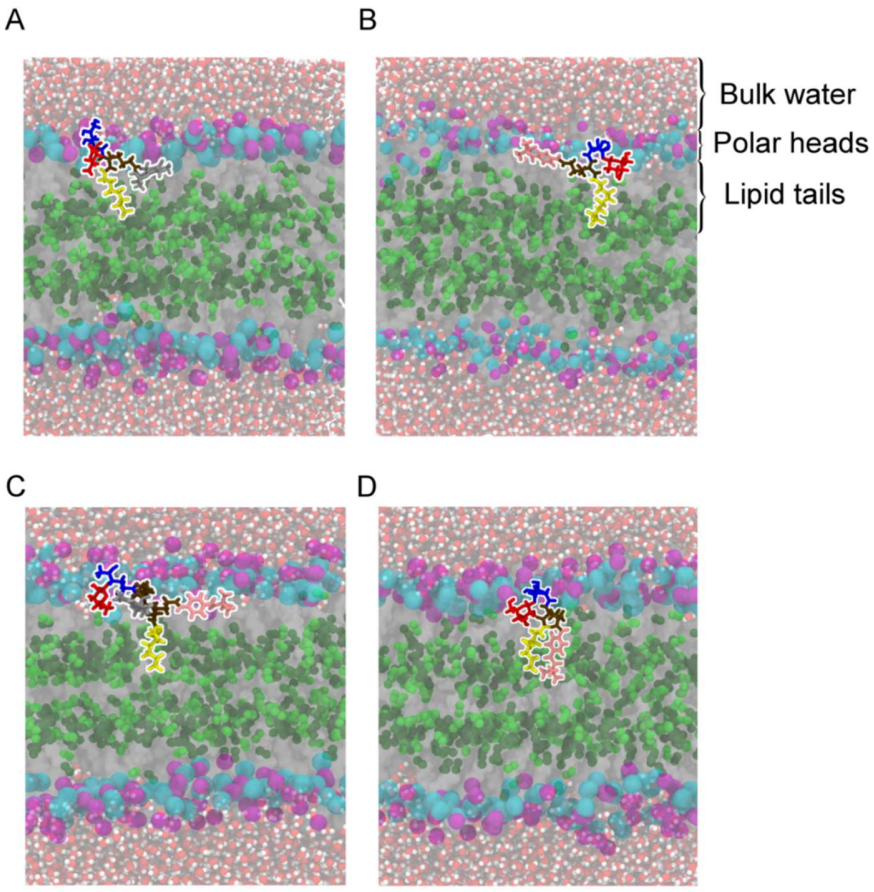

Fig. 7. Representative snapshots of the preferred location of FATx (A), FAPBN (B) and FATxPBN (C). Fig. 6D depicts the minor conformation of FAPBN, in which the PBN moiety is lined up along the fluorinated chain. The 1LB (β-D-Galactose), GA4 (gluconic acid), DAH (2,6-diaminohexanoic acid) and DFA (3,3,4,4,5,5,6,6,7,7,8,8,8-dodecafluorooctan-1-amine) moieties are depicted in red, blue, brown and yellow, respectively. Trolox and PBN are depicted in grey and pink, respectively. The cholines are depicted in cyan, the phosphates are depicted in magenta, 1st and 2nd unsaturations are depicted in green and dark-green, respectively.

Table 1. Binding parameters and rate of penetration (k) of the fluorinated antioxidants in DLiPC monolayers.

	FATxPBN	FATx	FAPBN
MIP (mN/m)	52.2 ± 2.3	48.6 ± 5.3	37.6 ± 5.3
$\Delta\Pi_{30}$ (mN/m)	10.0 ± 0.4	9.0 ± 1.5	2.1 ± 1.1
Synergy factor	0.55 ± 0.02	0.52 ± 0.06	0.71 ± 0.05
k (s^{-1})	$1.11*10^{-2}$	$1.17*10^{-2}$	$0.52*10^{-2}$

Table 2. Positions given as distances from the middle of the bilayer (in Å) of key moieties of DLPC (*i.e.,* choline, phosphates, unsaturations) and the different derivatives Trolox, Anionic Trolox, PBN, FATx, FAPBN, minor conformer of FAPBN (FAPBN*) and FATxPBN (*i.e.,* Trolox moiety, Trolox OH-phenolic, PBN, PBN amine moiety, 1LB = β-D-Galactose, GA4 = gluconic acid; DAH = 2,6-diaminohexanoic acid, DFA = 3,3,4,4,5,5,6,6,7,7,8,8,8-dodecafluorooctan-1-amine), as well as center-of-mass (COM) of the three fluorinated antioxidants FATx, FAPBN and FATxPBN. The positions were averaged over the second half of the MD simulations.

	Trolox	Anionic Trolox	PBN	FATx	FAPBN	FAPBN*	FATxPBN
Cholines	20.4 ± 0.4	20.3 ± 0.4	20.5 ± 0.4	20.5 ± 0.3	20.5 ± 0.3	20.5 ± 0.3	20.5 ± 0.3
Phosphates	19.1 ± 0.4	19.0 ± 0.4	19.2 ± 0.3	19.2 ± 0.3	19.2 ± 0.2	19.2 ± 0.3	19.2 ± 0.3
1st lipid unsaturation	7.2 ± 0.3	7.2 ± 0.3	7.2 ± 0.3	7.2 ± 0.2	7.3 ± 0.2	7.3 ± 0.2	7.2 ± 0.2
2nd lipid unsaturation	5.6 ± 0.2	5.6 ± 0.2	5.7 ± 0.2	5.7 ± 0.2	5.7 ± 0.1	5.7 ± 0.2	5.7 ± 0.2
Trolox	14.0 ± 1.7	15.3 ± 1.8		14.0 ± 2.3			13.9 ± 1.7
Trolox phenolic OH group	15.1 ± 2.2	14.2 ± 2.2		14.7 ± 2.6			14.0 ± 2.3
PBN			13.6 ± 2.7		15.7 ± 2.5	9.0 ± 2.1	13.8 ± 1.5
PBN amine			13.8 ± 2.8		15.2 ± 2.9	7.4 ± 2.0	13.9 ± 1.8
1LB				16.7 ± 1.7	16.3 ± 2.0	17.6 ± 1.7	16.8 ± 1.9
GA4				20.4 ± 1.5	20.0 ± 1.9	20.9 ± 1.8	19.6 ± 1.7
DAH				16.3 ± 1.9	16.2 ± 1.8	16.1 ± 2.1	15.2 ± 1.2
DFA				10.0 ± 1.8	10.4 ± 1.9	11.1 ± 1.9	8.2 ± 1.6
FATx COM				14.3 ± 1.7			
FAPBN COM					14.7 ± 1.7	13.9 ± 1.8	
FATxPBN COM							13.7 ± 1.1

Table 3. Combination index (CI) of FATx and FAPBN. CI<1: supra-additive, CI=1: additive, CI>1: infra-additive. Values with different superscripts differ significantly ($p < 0.05$).

Concentration (µM)	Combination index	Effect
0,4	0,46[a]	Supra-additive
0,6	0,69[a]	Supra-additive
0,8	0,92[a]	Supra-additive
1,6	1,83[b]	Infra-additive
3,2	3,66[b]	Infra-additive
6,4	7,33[b]	Infra-additive
12,8	14,66[b]	Infra-additive
25,6	29,31[b]	Infra-additive
38,4	43,97[b]	Infra-additive

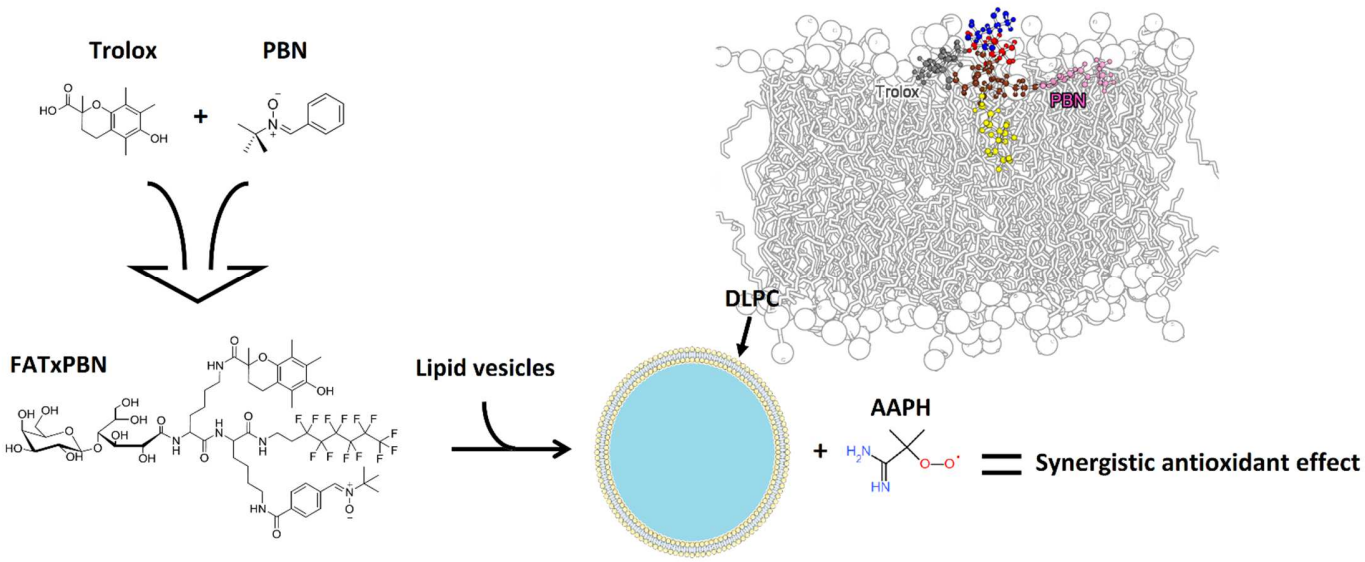
Trolox
PBN
FATxPBN
Lipid vesicles
DLPC
Trolox
PBN
AAPH
Synergistic antioxidant effect